STP 619

STRUCTURE, CONSTITUTION, AND GENERAL CHARACTERISTICS OF WROUGHT FERRITIC STAINLESS STEELS

J. J. Demo

AMERICAN SOCIETY FOR TESTING AND MATERIALS

WROUGHT FERRITIC STAINLESS STEELS

04-619000-02

STP 619

STRUCTURE, CONSTITUTION, AND GENERAL CHARACTERISTICS OF WROUGHT FERRITIC STAINLESS STEELS

Sponsored by
Committee A-1 on
Steel, Stainless Steel, and Related Alloys

by J. J. Demo

ASTM SPECIAL TECHNICAL PUBLICATION 619

List price $7.50
04-619000-02

AMERICAN SOCIETY FOR TESTING AND MATERIALS
1916 Race Street, Philadelphia, Pa. 19103

Library of Congress Catalog Card Number: 76-42961

NOTE

Reprinted by permission from the
Handbook of Stainless Steels
edited by D. Peckner and I. M. Bernstein
McGraw-Hill Book Company, New York

Printed in Baltimore, Md.
January 1977

Foreword

This special technical publication appears as Chapter 6 of *Handbook of Stainless Steels* published by McGraw-Hill Book Company and is reprinted here by permission. Committee A-1 on Steel, Stainless Steel, and Related Alloys of the American Society for Testing and Materials is the sponsor of this publication.

Related
ASTM Publications

Bearing Steels: The Rating of Nonmetallic Inclusion, STP 575 (1975), $27.25 (04-575000-02)

Cleaning Stainless Steel, STP 538 (1973), $18.00 (04-538000-02)

Introduction to Today's Ultrahigh-Strength Structural Steels, STP 498 (1971), $3.75 (04-498000-02)

A Note of Appreciation to Reviewers

This publication is made possible by the authors and, also, the unheralded efforts of the reviewers. This body of technical experts whose dedication, sacrifice of time and effort, and collective wisdom in reviewing the papers must be acknowledged. The quality level of ASTM publications is a direct function of their respected opinions. On behalf of ASTM we acknowledge with appreciation their contribution.

ASTM Committee on Publications

Editorial Staff

Contents

J. J. Demo[1]

STRUCTURE, CONSTITUTION, AND GENERAL CHARACTERISTICS OF WROUGHT FERRITIC STAINLESS STEELS

REFERENCE: Demo, J. J., *Structure, Constitution, and General Characteristics of Wrought Ferritic Stainless Steels, ASTM STP 619,* American Society for Testing and Materials, 1977.

ABSTRACT: High chromium-ferritic stainless steels have good general corrosion and pitting resistance and are resistant to stress-corrosion cracking. Despite these desirable properties, the alloys have found little use as materials of construction. This lack of use is a result of significant losses in ductility, toughness, and corrosion resistance when these alloys are subjected to moderate or high temperatures. Names given to the phenomena causing loss in properties include 475°C, sigma phase, and high-temperature embrittlement. This publication summarizes the literature describing the causes, the cures, and the limitations imposed on alloys when these problems occur. The most seriously limiting problem—high temperature embrittlement and loss or corrosion resistance—is discussed in considerable detail. The key role that interstitial carbon and nitrogen play on notch sensitivity and loss of ductility and corrosion resistance following a high-temperature exposure as in welding is defined. Good as-welded properties, the absence of which has severely restricted the use of ferritic stainless steels, depend on controlling interstitial carbon and nitrogen. The publication describes three methods that are being used for interstitial control. It is now possible to produce ferritic stainless steels which are tough and which have excellent corrosion resistance and ductility in the as-welded conditions. Several new high-chromium ferritic alloys with these desirable properties are being produced commercially.

KEY WORDS: ferritic stainless steels, embrittlement, sigma phase, properties, corrosion resistance, notch sensitivity, interstitial, stabilization

The high chromium-iron steels represent the fourth class of alloys in the family of stainless steels, the other three classes being austenitic, martensitic, and precipitation-hardening stainless and heat-resisting steels. Ferritic stainless steels are iron-based alloys containing from about 12 to 16

---

[1] Senior consultant, Materials Engineering, Engineering Service Division, Engineering Dept., E. I. du Pont de Nemours and Co., Inc., Wilmington, Del. 19898.

and 30 percent chromium. The high chromium limit is arbitrary and is meant simply to include all commercially produced alloys. Ferritic stainless steels, though known for more than 40 years, have had more restricted utility and less wide use than the austenitic stainless steels. Reasons for this include: the lack of the ductility characteristic of austenitic stainless steels, their susceptibility to embrittlement, notch sensitivity, and poor weldability, all factors contributing to poor fabricability. However, with the increasing cost of nickel, the high resistance of the ferritic steels to stress-corrosion cracking, and their excellent corrosion and oxidation resistance, intensive research over the decade of 1960's has resulted in ferritic alloy compositions which have good weldability and fabricability.

Structure and Constitution

In theory, the ferritic stainless steels are structurally simple. At room temperature, they consist of chromium-iron alpha (α) solid solution having a body-center-cubic crystal (bcc) structure. The alloys contain very little dissolved carbon; the majority of the carbon present appears in the form of more or less finely divided chromium carbide precipitates. They remain essentially ferritic or bcc up to the melting point. A typical constitution diagram, as published by the American Society for Metals [*1*][2] is reproduced in Fig. 1. Attention is directed to the lower chromium end of the phase diagram at the region of intermediate temperatures, about which several points can be stated.

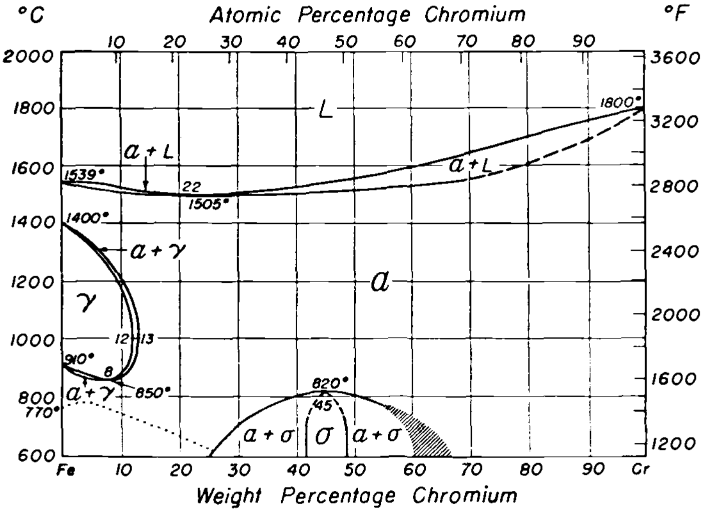

FIG. 1—*Chromium-iron phase diagram* [1].

---

[2] The italic numbers in brackets refer to the list of references appended to this paper.

1. Chromium is a member of a group of elements called ferrite formers which extend the α-phase field and suppress the gamma (γ)-phase field. This property results in the so-called γ loop extending in a temperature range from 850 to 1400°C.
2. As shown in Fig. 1, the transformation in chromium-free iron from α to γ phase occurs at about 910°C. As chromium is added, the transformation temperature is depressed to about 850°C at 8 percent chromium and then rapidly increased so that, at 12 to 13 percent chromium, the transformation temperature is about 1000°C.
3. The transformation from γ to α which occurs at about 1400°C for pure iron is depressed with increasing chromium to about 1000°C at 12 to 13 percent chromium. At this point, the upper and lower temperature curves for transformation join up to close off and form the γ loop. Beyond 12 to 13 percent chromium, transformation to γ is no longer possible, and an alloy would remain ferritic or bcc all the way from below room temperature to the melting point. It will be seen that this maximum limit for the existence of γ phase is very much a function of austenitizing elements and can be moved to higher chromium levels in the presence of these elements, particularly the interstitials carbon and nitrogen. For alloys with less than about 12 percent chromium, an $\alpha \rightarrow \gamma$ transformation occurs on heating into the γ range just as in pure iron. Ferritic stainless steels cannot normally undergo this transformation upon heating and cooling.
4. Between the γ loop and α-phase field, there is a narrow transition region where an alloy at temperature will have both α and γ phases which, depending on the quench rate, may or may not be retained at room temperature.

Effect of Carbon and Nitrogen

The location of the γ loop in the iron-chromium phase diagram has been carefully studied recently by Baerlecken, Fischer, and Lorenz [*2*]. These investigators used magnetic measurements at elevated temperatures to determine the effect of carbon and nitrogen (and nickel) on the formation of austenite. The detailed α and γ regions these workers developed for pure iron and chromium alloys are shown in Fig. 2. The lowest point in the γ loop occurs at 840°C and 6.5 percent chromium. The greatest width of the two-phase field is at about 1075°C, and the complete enclosure is reached at about 11.5 percent chromium. Since the greatest expansion of the γ region is to about 10.6 percent chromium, the two-phase $\gamma + \alpha$ region is very narrow in this high-purity alloy.

Additions of austenitizing elements, particularly carbon and nitrogen, cause the outside boundary of the $\gamma + \alpha$ two-phase field to shift to higher chromium levels. The powerful effects of carbon and nitrogen in this

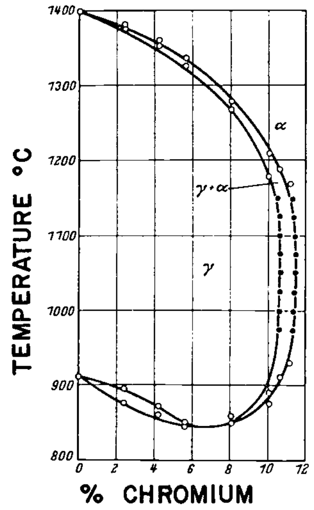

FIG. 2—*Iron loop of the iron-chromium phase diagram for alloys with about 0.004 percent carbon and 0.002 percent nitrogen* [2].

regard are shown in Figs. 3*a*,*b* taken from work by Baerlecken et al [2]. Two effects are observed: namely, an expansion of the two-phase region to higher chromium contents and the shifting of the maximum extension of the γ + α phase field to higher temperatures. For example, it is seen in Fig. 3*a* that 0.013 percent carbon and 0.015 percent nitrogen shift the maximum expansion of the γ + α from 11.5 to 17.0 percent chromium, while 0.04 percent carbon and 0.03 percent nitrogen shift it to about 21 percent chromium. At still higher carbon levels, for example, 0.2 percent,

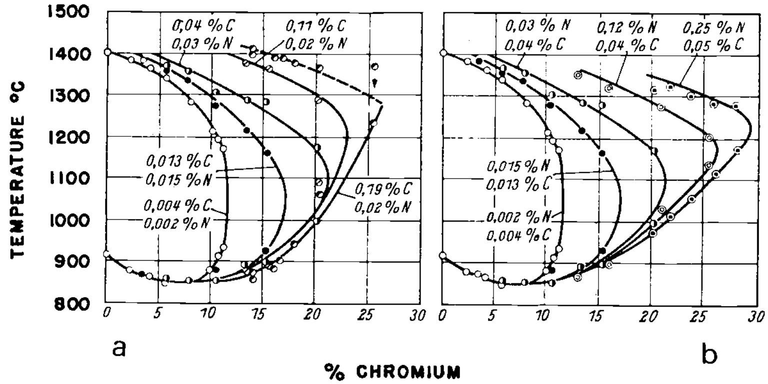

FIG. 3—*Shifting of the boundary line* (γ + α)/α *in the system iron-chromium through increasing additions of carbon or nitrogen* [2].

an expansion to 26 percent chromium is observed. In addition, the point of greatest expansion of the two-phase region is shifted to higher temperatures, from about 1075°C for the pure alloy to about 1300°C for an alloy containing 0.2 percent carbon. The expansion of the two-phase region to even higher temperatures is limited by the solidus temperatures of the alloys. As evident from Fig. 3*b*, nitrogen acts similar to carbon as a powerful expander of the two-phase $\gamma + \alpha$ field. In an alloy containing 0.25 percent nitrogen, the point of greatest width of the two-phase field is shifted from 11.5 percent chromium for the pure alloy to 28 percent chromium and to higher temperatures, from 1075 to about 1250°C.

Besides its effect on extending the two-phase $\gamma + \alpha$ region, carbon, because of its low solubility in the α matrix, is rejected from solid solution as complex carbides, $(Cr,Fe)_7C_3$ and $(Cr,Fe)_{23}C_6$ which precipitate predominantly at the grain boundaries [*3,4*]. When an alloy is heated to temperatures of 1100 to 1200°C and the carbon level exceeds about 0.01 percent [*2*], the carbon cannot be held in solid solution even with rapid quenching, and the complex carbides are formed, which drastically affect the properties of the alloys.

It is at once obvious from this that whether or not an alloy remains completely bcc depends very much on the chromium and the interstitial levels. At low-chromium levels, even alloys with relatively low interstitial levels may have a duplex structure when heated to temperatures around 1100°C. Alloys at the higher chromium levels can only have a duplex structure if they also contain high interstitial levels; otherwise, these alloys are fully ferritic at all temperatures. In general, beyond about a 13 percent chromium content, heating to high temperatures no longer produces massive transformation of α to γ; therefore, grain refinement and hardening by heat treatment and quenching are no longer possible.

Strengthening Mechanisms

As just described, the ferritic stainless steels are characterized by the essential absence of the α to γ transition upon heating to high temperatures. Consequently, hardening by the γ to martensite transition upon cooling will not normally occur. This transformation mechanism is utilized in carbon and alloy steels and martensitic chromium-iron alloys for achieving high hardness and strengths. The influence of heat treatment temperature on hardness for two ferritic stainless steels and a martensitic stainless steel are depicted in Fig. 4, based on data from Refs *5* and *6*. In contrast to the 13 percent martensitic steel which undergoes the $\alpha \rightarrow \gamma \rightarrow$ martensite transition, the hardness on an 18 and 20 percent chromium steel varies little with temperature. The fact that there is some hardening occurring is due to the small amount of austenite formed at temperature which is dependent upon the chromium content and inter-

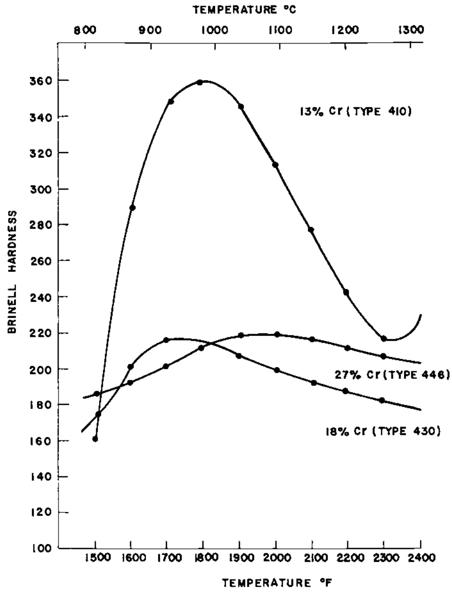

FIG. 4—*Relative hardening of ferritic and martensitic chromium-iron alloys after water quenching from indicated temperature* [5,6].

stitial levels. For ferritic stainless steels, the hardening effect is strongest at the lower chromium ranges but can occur even at higher chromium levels if the carbon content is increased so as to expand the α to γ, two-phase region as shown in Figs. 3*a*,*b*.

In summary, it is not possible to harden or strengthen ferritic stainless steels significantly by heating them to high temperatures and cooling rapidly. In these alloys, the slight increases in hardness or strength when the alloys are heated above 850°C are related to increases in grain size (through grain growth) and the presence of small volumes of austenite which reverts to martensite upon cooling.

Strengthening by Heat Treatment

Though a ferritic iron-chromium stainless steel cannot be strengthened or hardened by the classical $\alpha \rightarrow \gamma \rightarrow$ martensite mechanism, the alloys are susceptible to significant strengthening by heat treatment. In general, the strengthening mechanisms that do occur are not desirable because the alloys are embrittled, and ductility and toughness at room temperature are severely reduced. Distinction will be made between three separate and distinct forms of embrittling mechanisms: (*a*) sigma (σ)-phase precipitation, (*b*) 475°C embrittlement, and (*c*) high-temperature embrittlement.

Surveys by Thielsch [*6*], Rajkay [*7*], Kaltenhauser [*8*], and Demo and Bond [*9*] have summarized the extensive literature, describing these embrittling phenomena. These effects have been major deterrents to the use of ferritic stainless steels as engineering materials. Because of their importance to engineering properties, a summary of each of these embrittling effects is given here with details as to the nature and cure of each.

Sigma Phase—This occurs in iron-chromium alloys containing between 15 to 20 and 70 percent chromium exposed to temperatures from about 500 to 800°C.

475°C Embrittlement—This embrittlement occurs when a ferritic iron-chromium stainless steel is heated between 400 and 540°C. An increase in hardness and tensile strength is observed, concurrent with a substantial decrease in ductility and impact resistance.

High-Temperature Embrittlement—This embrittlement derives its name from the fact that ferritic alloys with moderate to high carbon and nitrogen levels are brittle at room temperature following exposure of the alloys to temperatures above about 1000°C.

While all these embrittling phenomena can affect severely the mechanical properties of a ferritic chromium-iron stainless steel in an engineering application, one is particularly serious, namely, high-temperature embrittlement. This effect is serious because a useful engineering material must be capable of being welded and heat treated while maintaining ductility, toughness, and corrosion resistance.

Sigma Phase

Examination of the phase diagram in Fig. 1 shows a second zone at lower temperatures centered about 45 percent chromium in addition to the γ loop. A detailed part of the σ portion of the chromium-iron phase diagram by Cook and Jones [*10*] is shown in Fig. 5. Pure σ forms between 42 and 50 percent chromium, while a duplex structure of both α and σ phases has been found to form in alloys with as little as 20 and as much as 70 percent chromium when they are exposed to temperatures between 500 and 800°C. The existence of a compound in the iron-chromium system at about 50 percent chromium was suggested as early as 1927 [*11,12*]. It was not until 1936 that the intermetallic compound, iron-chromium, was definitely identified as σ phase [*13,14*]. σ phase is an intermetallic compound containing one atom of iron with one atom of chromium which is hard, nonmagnetic, and consists of a tetragonal unit cell. Extensive research has been reported describing the effort to establish the structure and transformation characteristic of this iron-chromium compound [*15-20*]. σ phase forms in other alloy systems when two metals with a bcc and face-centered-cubic (fcc) structure are alloyed together

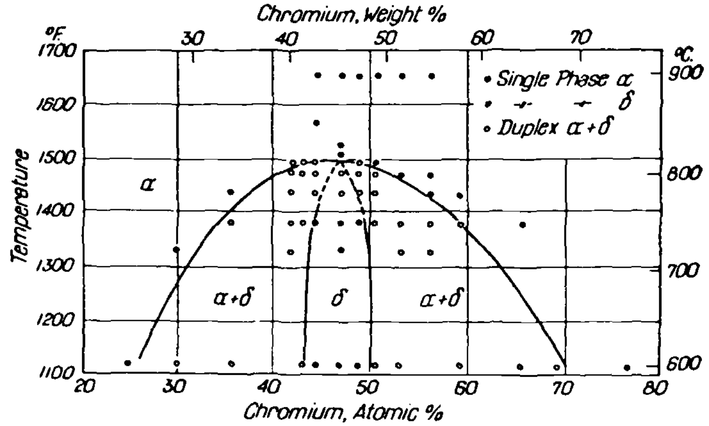

FIG. 5—*Iron-chromium phase diagram in binary high-purity 25 to 76Cr alloys. This diagram shows pure σ phase from 44 to 50 percent chromium and mixed α and σ phase from about 25 to 44 and from 50 to 70 percent chromium with phase boundaries for temperature interval of 1100 to 1500°F (595 to 815°C)* [10].

and have atomic radii not differing by more than 8 percent [*3*]. Elements like molybdenum, silicon, nickel, and manganese shift the σ-forming range to lower chromium content [*3,13,14,20,21*]. σ phase forms readily on heating alloys containing 25 to 30 percent chromium to 600°C but only after a relatively long-time exposure. In alloys containing less than about 20 percent chromium, σ phase is difficult to form [*3*]. Cold work enhances the rate of σ-phase precipitation [*14,19,21-24*]. The formation of σ phase is accompanied by an increase in hardness and a severe reduction in ductility and toughness [*25*], especially when these properties are measured at ambient temperatures. An important consideration is that, in most chromium-iron alloys, σ forms very slowly, requiring hundreds of hours. This is shown by the data in Fig. 6 from Shortsleeve and Nicholson [*20*] describing the threshold times of σ formation at 595 and 650°C as a function of chromium content. Based on these data, weld deposits and casting normally would not have sufficient time in the appropriate temperature ranges for σ to form in alloys, especially those containing 15 to 33 percent chromium [*6*]. Only with long isothermal holds can σ phase form to severely reduce the ductility and toughness of chromium-iron alloys. A representative microstructure [*25*] of a 27Cr alloy exposed for 3144 h at about 540 to 565°C shows a structure composed of ferrite, spheroidized carbides, and σ phase (Fig. 7). The σ phase has been precipitated as an essentially continuous series of islands around the ferrite grain boundaries. Under some exposure conditions, these islands are preferentially attacked (Fig. 7*c*) indicating that the presence of σ phase is also detrimental to the corrosion resistance of

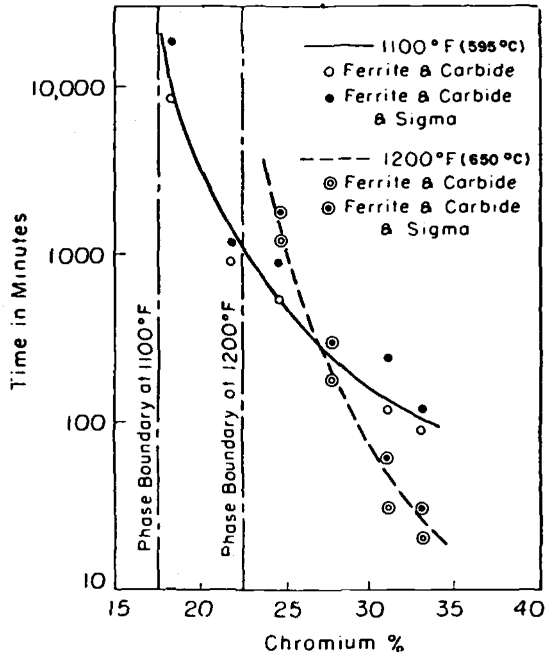

FIG. 6—*Effect of chromium content on the threshold times of σ formation at 1100 and 1200°F (595 and 650°C)* [20].

chromium-iron alloys. Fortunately, σ phase developed in an alloy may be brought into solution with relatively short holding periods of an hour or more by heating at a temperature over 800°C [*6*]. Alloys containing nickel, molybdenum, and manganese may require longer holding periods or higher temperatures to dissolve σ phase.

475°C Embrittlement

When chromium-iron alloys containing 15 to 70 percent chromium are subjected to prolonged heating at temperatures between 400 and 540°C, the alloys harden, and a drastic loss in ductility is observed. The hardening phenomenon is referred to as 475°C (885°F) embrittlement because peak hardness on aging occurs at this temperature, as illustrated in Fig. 8 [*6,25*] for chromium-iron stainless steels heated for long times at selected temperatures. The effect of prolonged heating at 475°C on increasing the strength and decreasing the ductility in an Fe-27Cr alloy is shown in Fig. 9 from the work of Newell [*25*]. As suggested by these data, hours of exposure at 475°C are required before noticeable changes in hardness and tensile properties are observed. However, notched specimens may reveal this embrittlement in a much shorter time. Zapffe et al

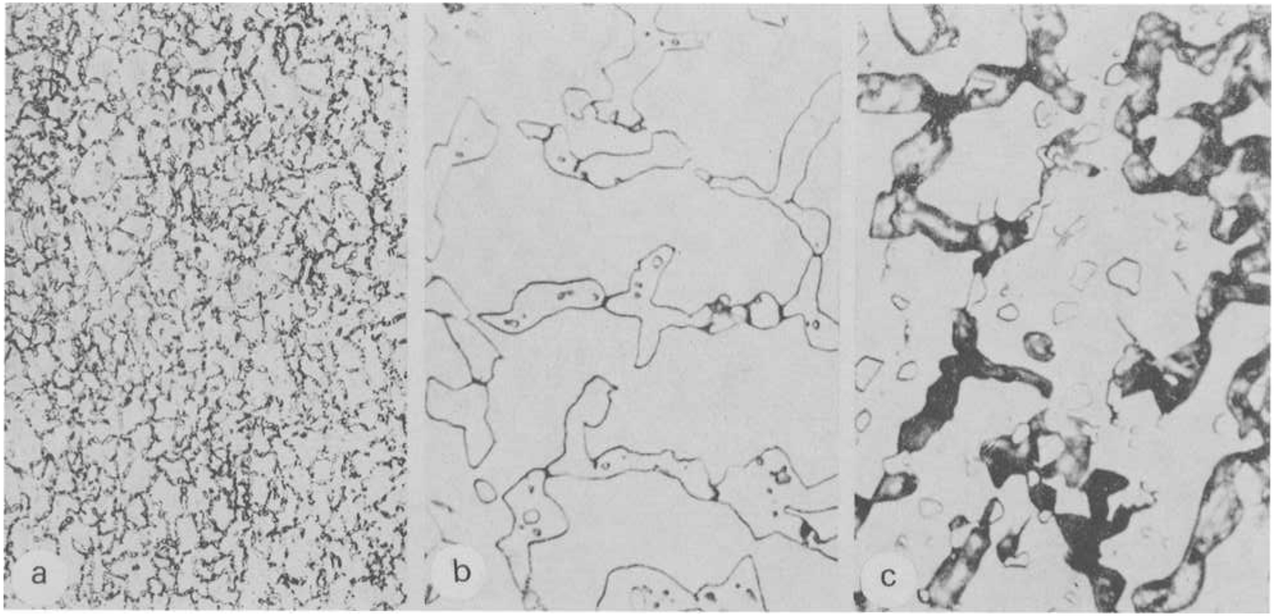

FIG. 7—(a) *27Cr-Fe alloy (air melted) showing ferrite, carbides, and intergranular σ-phase constituent formed after heating 131 days at approximately 1050°F (565°C)* (~ ×*200*). (b) *σ phase with some small spheroids of carbides around which σ phase has been formed* (~ ×*1000*). (c) *Etched 10 s in aqua regia during which σ phase is blackened and eaten out. Carbides appear mainly in center of ferrite grains* (~ ×*1000*) [25].

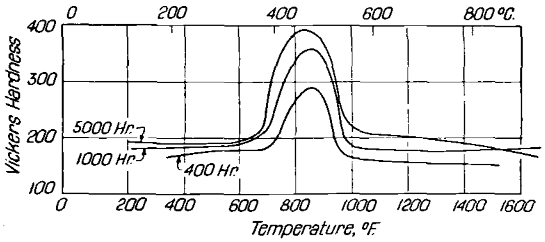

FIG. 8—*Hardness surveys on bars after prolonged heating in a temperature gradient. Analysis: 0.20 percent maximum carbon, 1.50 percent maximum manganese, 0.025 percent maximum sulfur and phosphorus, 0.75 percent maximum silicon, 26 to 30 percent chromium, 1.00 percent maximum nickel, 0.12 to 0.25 percent nitrogen* [25].

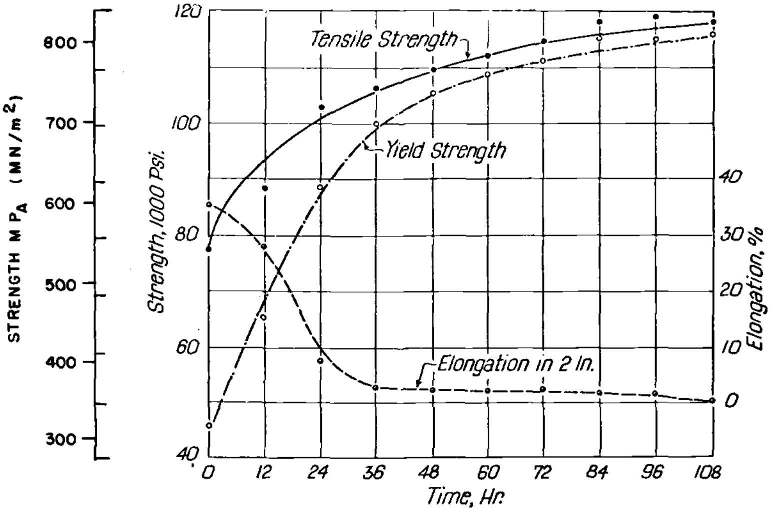

FIG. 9—*Graph showing effect of aging time at 885°F (475°C) on room-temperature tensile properties of 27Cr-Fe alloy, air melted* [25].

[*24,26*], using a 26Cr stainless steel, were able to show embrittlement on notch specimens in a bend test after only the first half hour of exposure at 475°C.

Large reductions in impact strength may also be noticed after only short-time exposure to embrittling temperature. Data taken from Colombier's book [*3*] are summarized in the following table to illustrate this point for a steel with 0.08 percent carbon, 0.4 percent silicon, and 16.9 percent chromium. The mechanical properties (tensile strength, yield strength, and elongation) show essentially no effect of the embrittling treatment, but a drastic loss in impact strength is recorded. As noted by

	Annealed	Heated 4 h at 450°C
Tensile, tsi[a]	37.0	38.0
Yield point, tsi	21.0	25.4
Elongation, %	22.8	23.6
Impact values, kg/cm²	12.0	1.4

[a] tsi = tons per square inch.

Colombier, after repeated heating in the range of 450 to 500°C, the elongation starts to decrease and, after a few hundred hours, may be virtually zero, while an increase in tension of some 7 to 8 tsi occurs.

The cause for the increase in strength and hardness and drastic reduction in ductility was unexplained for a long time. X-ray diffraction analysis by Becket [*27*], Riedrich and Loib [*28*], and Bandel and Tofaute [*29*] on specimens embrittled by heating in the neighborhood of 475°C showed no changes in lattice parameter. Newell [*25*], while reporting no changes in lattice parameters, did note that an atomic disturbance was occurring because the diffraction lines in back-reflection spectra of an embrittled specimen were diffuse and broad. Early investigators could detect no significant change in metallographic features, although Riedrich and Loib [*28*] and Newell [*25*] did report a grain boundary widening. Based on this observation, Riedrich and Loib concluded that the embrittlement was caused by a precipitate along the grain boundary. In separate work, Bandel and Tofaute [*29*] discovered that an embrittled 18Cr alloy had a lamellar precipitate. Prior to 1951, 475°C embrittlement was considered to be related to σ-phase formation and received the attention of many studies. Newell [*25*] in 1946 showed that the embrittlement would occur in practically carbon-free alloys as well as in those of moderate carbon content. Bandel and Tofaute [*29*], Riedrich and Loib [*28*], and Newell [*5*] showed that the degree of hardening as a function of temperature exposure was proportional to chromium content. The data from Riedrich's and Loib's work using experimental low-carbon alloys are produced in Table 1. The alloys in the annealed condition at the start

TABLE 1—*Hardnesses[a] of chromium-iron alloys after 1000 h exposure at 885°F (475°C) as a function of chromium content.*

Chromium, % by weight	Brinell Hardness	Chromium, % by weight	Brinell Hardness
14.5	150	20.1	260
15.9	195	21.9	270
17.0	223	23.7	290
19.4	252	28.7	320

NOTE—Data by Newell [*5*] and Riedrich and Loib [*28*].

[a] The hardness of annealed alloys at the start was about 145 Brinell.

all measured about 145 Brinell. The hardnesses after 1000-h exposure at 475°C are tabulated in the table. N. D. Newell's [5] data reproduced in Fig. 10 also show the relationship of chromium content in commercial alloys to hardness increases. Rapid increases in hardness with exposure times were noted for Types 446 and 430 stainless steel, with little change noted for Types 410 and 405 stainless steel (12 percent chromium). These data indicate that the hardening occurs in alloys containing over about 15 percent chromium, increases with chromium content, and is particularly pronounced for a commercial Type 446 stainless steel containing 26 percent chromium.

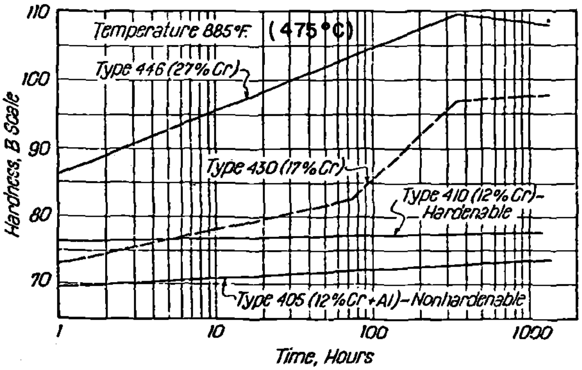

FIG. 10—*Age hardening tendencies at 885°F (475°C) of 12, 17, and 27Cr-Fe alloys* [5].

In 1951, Heger [*30*] emphasized the suggestion first made by Bandel and Tofaute [*29*] and Newell [*5*] that the embrittlement was due to a precipitation hardening process involved in the early stages of formation of σ phase. This was in contrast to the theory of a minor impurity precipitation which was rendered untenable because alloy additions [*30*] and prior heat treatment [*29*] did not improve resistance to the embrittlement, and even the purest chromium-iron alloys embrittled [*27*]. The cause, as put forth by Heger [*30*] and Newell [*5,25*], was precipitation of some phase which is inherent in the chromium-iron alloy system itself and not an impurity. Heger postulated that 475°C embrittlement occurred when a chromium-iron alloy heated in the embrittling range undergoes the reaction

$$\alpha \text{ phase} \rightarrow \text{transition phase} \rightarrow \sigma \text{ phase}$$

The transitory phase that proceeds σ formation at higher temperature was said to cause 475°C embrittlement. Newell described the embrittlement phenomenon as being related first to an initial lattice change or distortion in the α matrix leading subsequently to gross precipitation of σ phase when the atomic mobility is increased at but slightly higher temperatures. As Heger pointed up, the transition phase is intermediate in structure between α and σ and is coherent with the matrix α phase. The presence of this coherency between the two different structures causes large resistance to dislocation motion typical of a precipitation-hardening mechanism [*31*]. The generated stresses then increase the hardness and cause other property changes. While both Heger and Newell felt 475 °C embrittlement was related to a transition state before σ phase is formed, Heger pointed up a very serious contradiction of this hypothesis. Houdremont's [*6,32*] data reproduced in Fig. 11 illustrate this problem. The alloys containing 17 and 28.4 percent chromium did not reveal any hardening because of σ-phase formation (600 to 900 °C). However, significant hardening in the 475 °C embrittlement range (400 to 550 °C) did occur. It thus appeared that 475 °C embrittlement phenomenon is definitely inherent to the chromium-iron binary system, as suggested by Heger and Newell, but it is not related directly to the formation of σ phase as postulated.

Based on extensive research work from 1951 to 1964, two hypotheses have been suggested to describe the mechanism of 475 °C embrittlement. One school—Masumota, Saito, and Sugihara [*33*] and Pomey and Bastien [*34*]—have attributed the changes in physical properties of alloys with aging at about 475 °C to atomic ordering. In fact, Takeda and Nagai [*35*] claimed to have found X-ray verification for super lattices corresponding to Fe_3Cr, FeCr, and $FeCr_3$. However, all published attempts to observe super lattices in chromium-iron α alloys using more sensitive neutron diffraction have been unsuccessful [*36–38*]. The second and more prevalent school of thought for the occurrence of 475 °C embrittlement is the formation of a coherent precipitate due to the presence of a miscibility gap in the chromium-iron system below about 550 °C, in a chromium range where σ phase can form at higher temperatures. The data published by Fisher, Dulis, and Carroll in 1953 [*39*] gave the first indication of the presence of a coherent precipitate. These investigations were able to extract fine particles about 200 Å in diameter from a 28.5Cr alloy aged for 1 to 3 years at 475 °C. The material was found to be nonmagnetic, to have a bcc structure with a lattice parameter ($a = 2.877$ Å) which is between that of iron and chromium, and to contain chromium in the range from 61 to 83 percent. Williams and Paxton [*40*] and Williams [*37*] confirmed these results and were the first to propose explicitly the existence of a miscibility gap below the σ-forming region in the equilibrium diagram of Fig. 1. The extent of the miscibility gap is shown in Fig. 12 as published by Williams [*37*]. Alloys aged within the gap would separate into chromium-rich ferrite (α^1) and iron-rich ferrite (α). Reversion to the unaged condition occurs when the specimens are heated above

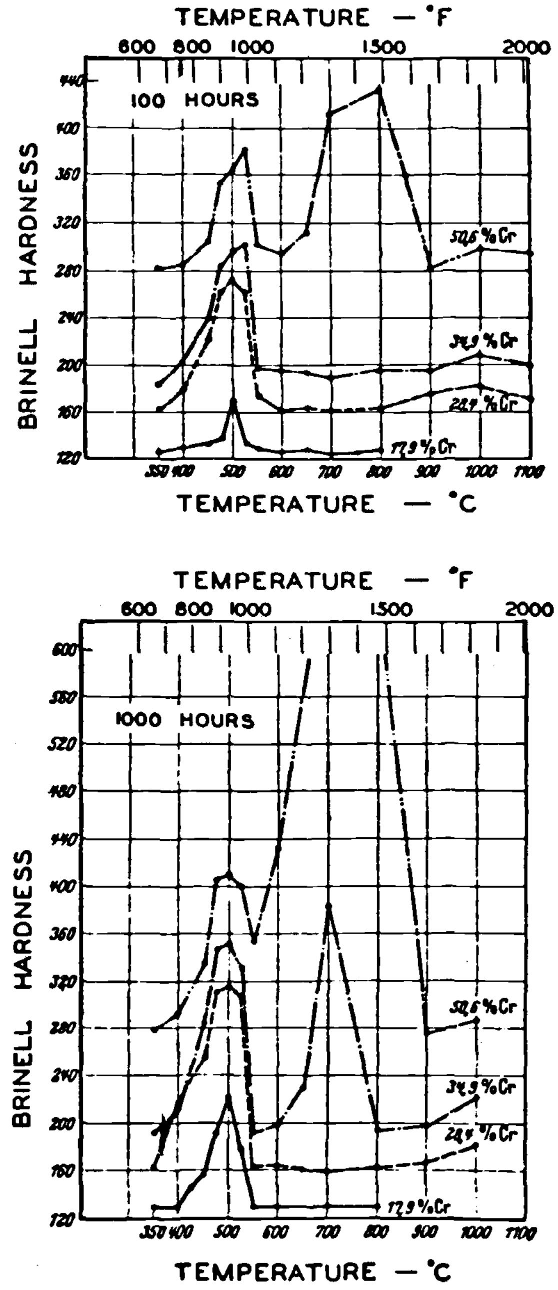

FIG. 11—*Effects of temperature and aging time on hardness increase caused by 885°F (475°C) brittleness and σ-phase precipitation in several chromium-iron alloys* [6,32].

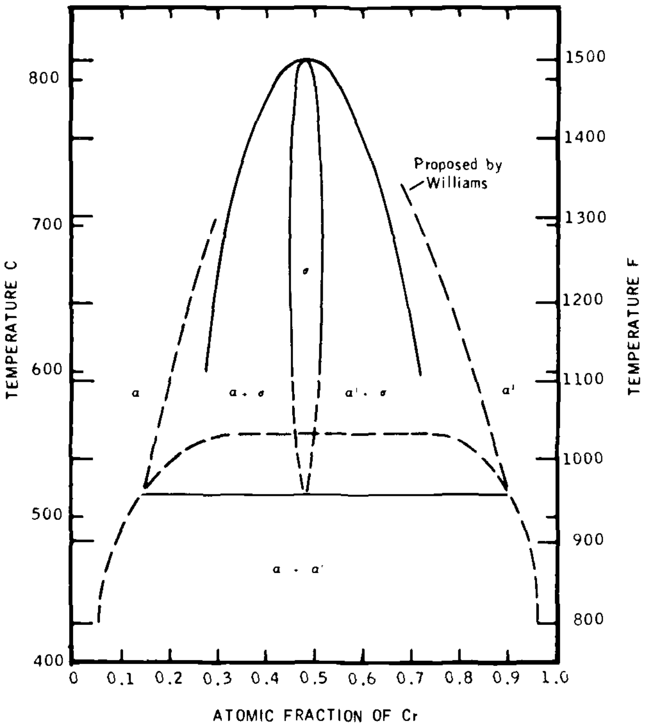

FIG. 12—*Phase diagram of the iron-chromium system according to Williams* [37].

550°C in agreement with all experimental data. The mechanism of age hardening by α–α^1 precipitation in the chromium-iron alloy system has been studied in detail by Marcinkowski, Fisher, and Szirmae [*41*] who analyzed the influence of the formation of a chromium-rich precipitate (α^1) on the deformation markings in the vicinity of hardness impressions. In addition, using extraction-replica and thin-foil transmission electron microscopy, these workers were able to show the existence of a coherent chromium-rich precipitate in an iron-rich matrix in a 46 percent by weight chromium-iron alloy heated for thousands of hours at 500°C (Fig. 13).

In more recent work on lower chromium content alloys, Grobner [*42*] established the critical temperature range as well as the kinetics of the embrittling process in chromium-iron alloys containing 14 and 18 percent chromium. He showed that, for an 18Cr alloy, 475°C embrittlement occurs in a temperature range from 400 to 500°C for both a commercial purity alloy and a low interstitial alloy. However, the vacuum-melted alloy of higher purity requires a longer exposure time to embrittle, as shown by Grobner's data on impact strength reproduced in Fig. 14. In addition to drastic changes in toughness, embrittled alloys, whether high

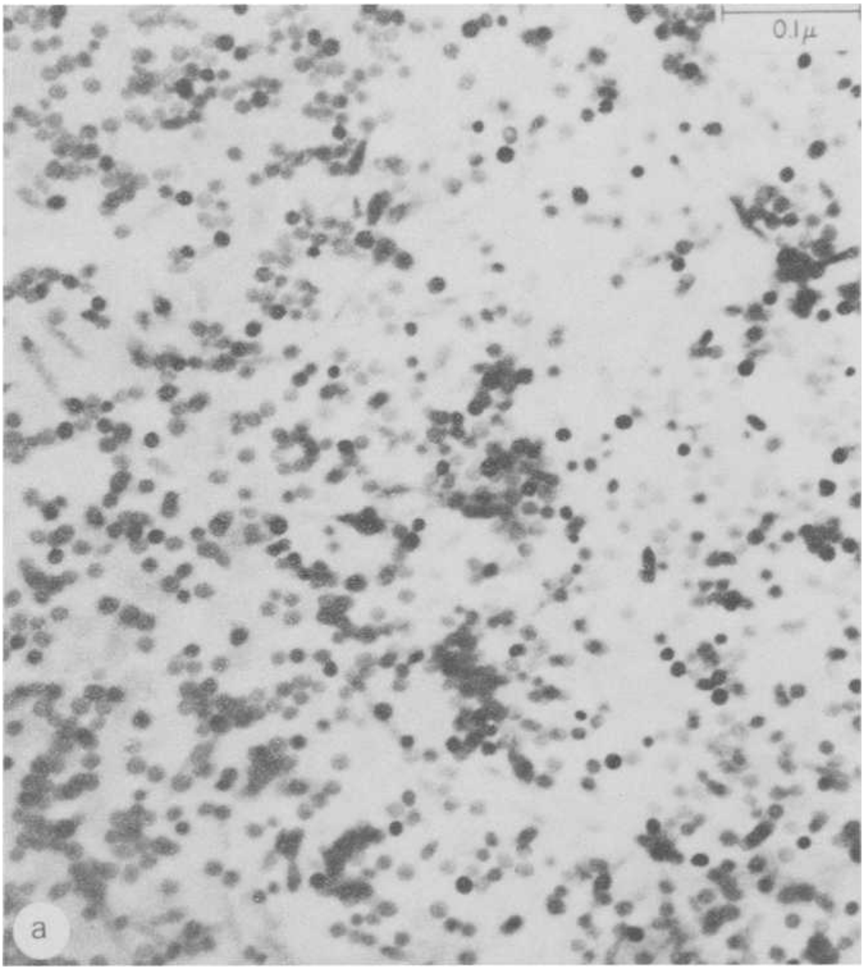

FIG. 13*a*—*Electron micrograph of an extraction replica of bcc chromium-rich zones existing in a 47.8 atomic percent chromium-iron alloy after annealing 9650 h at 500°C.*

purity and vacuum melted or air melted, show increases in yield and tensile strength and drastic reduction in elongation, as shown in Table 2. Finally, Grobner showed that even steels with chromium contents as low as 14 percent show embrittlement when exposed in the temperature range of 370 to 485°C, but only after much longer exposure times as compared to the 18Cr steels.

Many investigators have studied the effect of additives on 475°C embrittlement in chromium-iron steels [*3,6,27,29,30,42*]. Heger [*30*] noted that, in general, the addition of alloying elements offered little or no improvement in preventing the embrittlement. The effects of additives

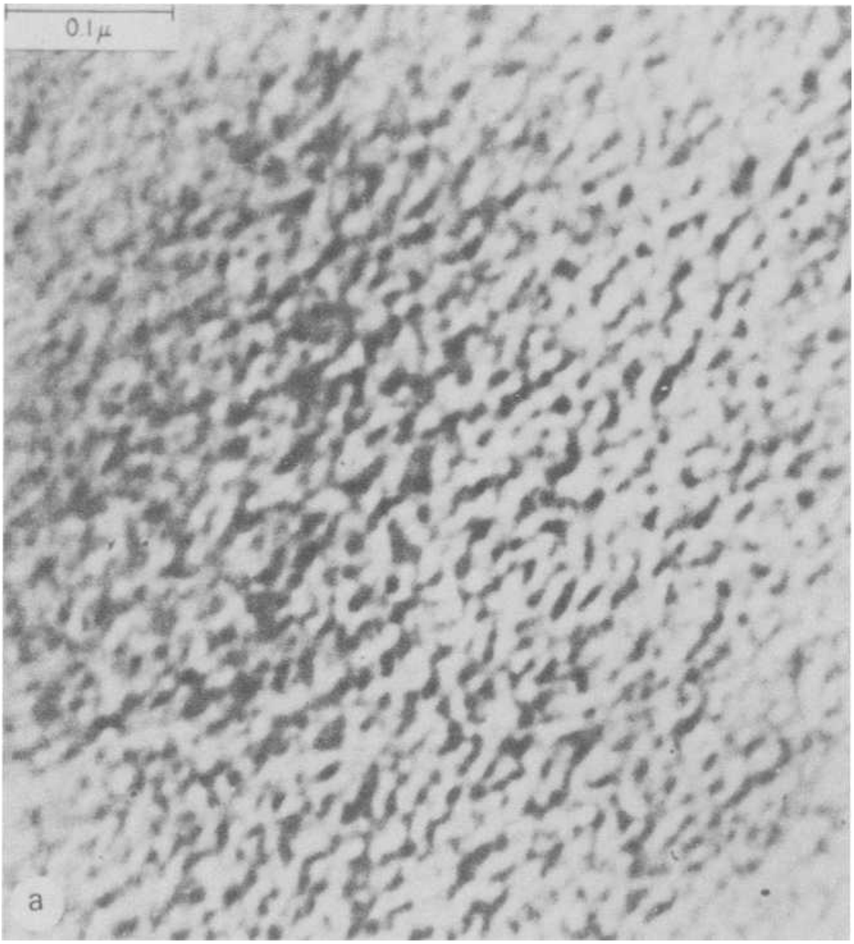

FIG. 13*b—Transmission electron micrograph showing structure existing in a 47.8 atomic percent chromium-iron alloy after annealing 3743 h at 500°C* [41].

on 475°C embrittlement taken from Heger [*30*] are summarized in Table 3. While not an additive, cold work [*6*] intensifies the rate of 475°C embrittlement. In addition to drastic reduction in toughness and ductility, embrittled chromium-iron alloys show a severe reduction in corrosion resistance [*24,29*]. Data from Newell's article [*24*], tabulated in Table 4, show that an embrittled alloy corrodes about four to twelve times more rapidly in boiling 65 percent nitric acid than does an annealed specimen. The accelerated corrosion on embrittled alloys is probably due to the selective corrosion of the iron-rich ferrite formed because of the miscibility gap or, as suggested by Hodges [*43*], due to formation of chromium-rich carbide precipitates.

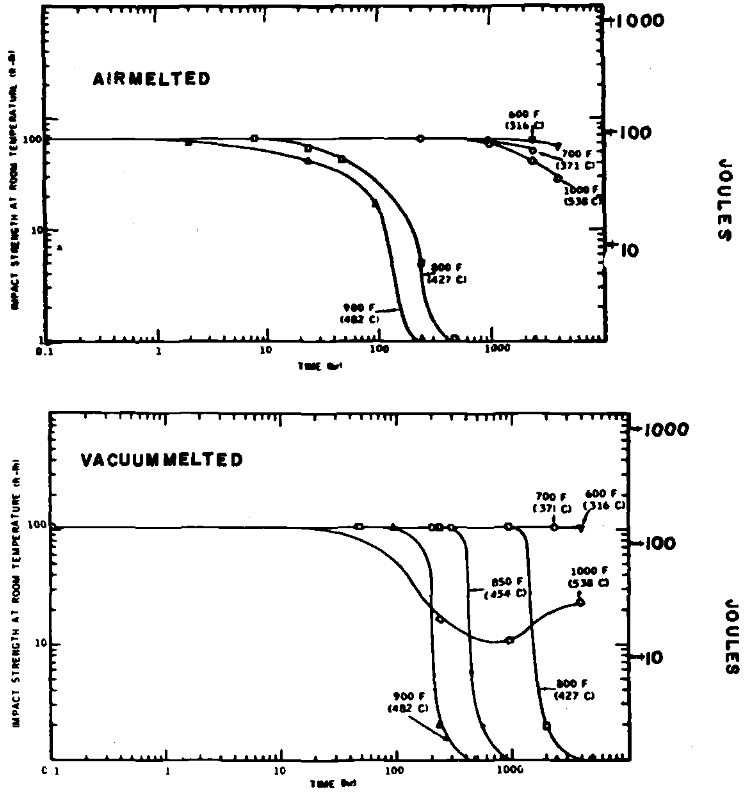

FIG. 14—*Impact strength at room temperature of half-size Charpy V-notch specimens after aging at indicated times and temperatures*; *air-melted versus vacuum-melted 18Cr alloys* [42].

The 475°C embrittlement may be alleviated and toughness and corrosion resistance restored by heating embrittled alloys at temperatures of 550°C and higher for a long enough time. As pointed up by Newell [*24*], 1 h suffices to remove the embrittlement at 593°C or higher, while 5 h are required at 582°C, and over 1000 h at 538°C. For compositions susceptible to σ-phase precipitation in a relatively short time, as indicated in Fig. 12, the 475°C embrittled alloy can be heated to temperatures above about 800°C (that is, above the σ-forming region) and rapidly cooled to remove the embrittlement [*6*].

Summary 475°C Embrittlement

Holding chromium-iron alloy in the temperature range of 400 to 540°C causes the alloys to become brittle and lose corrosion resistance. The

TABLE 2—*Tensile properties at room temperature of a vacuum-melted and air-melted alloy after indicated aging treatments.*

Alloy Type	Aged Temperature, °C	Aged Time, h	0.2% Offset Yield Strength, ksi (MPa)	Tensile Strength, ksi (MPa)	Elongation, % (50.8-mm gage)
1		0	30.9 (213)	49.9 (344)	32.5
1	316	4000	31.6 (217)	50.8 (350)	38.3
1	427	4800	69.8 (481)	84.1 (579)	13.0
1	482	2400	73.4 (505)	100.3 (690)	11.5
2		0	43.0 (296)	69.8 (481)	22.5
2	316	4000	38.5 (265)	69.1 (476)	25.5
2	427	960	73.7 (508)	95.8 (660)	17.0
2	482	2400	83.4 (540)	104.0 (717)	12.5

Alloy	Cr	C, % by weight	N
1 vacuum melted	17.4	0.002	0.003
2 air melted	18.0	0.044	0.091

NOTE—Data by Grobner [*42*].

TABLE 3—*Effects of composition on 475°C embrittlement in chromium-iron alloys.*

Element	Effect on 475°C Embrittlement[a]
Cr	intensifies
C	no effect[a]; intensifies[b]
Ti, Cb	intensifies
Mn	lowers slightly
Si	intensifies
Al	intensifies
Ni	low amounts; intensify large amounts; decrease
N	very slight[a]; intensifies[b]
P	intensifies
Mo	intensifies
Severe cold work	intensifies[c]

[a] Heger [*30*].
[b] Grobner [*42*].
[c] Thielsch [*6*].

TABLE 4—*Average rate of corrosion in boiling 65% nitric acid for 27Cr alloy after aging at 475°C.*

Condition	Corrosion Rates, mil/year
Annealed	8.9
Embrittled 500 h at 475°C	31
Embrittled 6000 h at 475°C	109

NOTE—Data by Newell [*25*].

embrittlement is caused by formation of coherent chromium-rich precipitate in the iron-rich matrix as a result of a miscibility gap in the chromium-iron phase diagram below about 550°C in the chromium range from about 15 to 70 percent. The 475°C embrittlement phenomenon and σ-phase embrittlement are not related metallurgically. Significantly shorter exposure times can cause 475°C embrittlement, as compared to σ-phase embrittlement. As with σ phase, it is unlikely that welding or a high-temperature heat treatment can produce 475°C embrittlement even if the alloy experiences a relatively slow cool through the embrittling temperature ranges. A very heavy section may suffer 475°C embrittlement during cooling. The fact that 475°C embrittlement or σ-phase embrittlement will not normally occur in alloys welded or annealed at high temperatures and then cooled makes these embrittling problems less serious. However, alloys with more than about 16 percent chromium should not be used for extended service between 370 and 540°C, especially if the alloy is cycled from room temperature to the operating temperature during process shutdowns or excursions.

High-Temperature Embrittlement and Loss of Corrosion

When high-chromium stainless steels of intermediate and high interstitial content are heated above about 950°C and cooled to room temperature, they may show a severe embrittlement [*31*] and loss of corrosion resistance [*44*]. The effects can occur during welding, isothermal heat treatments above 950°C, and casting operations. The effect on ductility and corrosion resistance is shown in Fig. 15 [*45*] for a commercial AISI

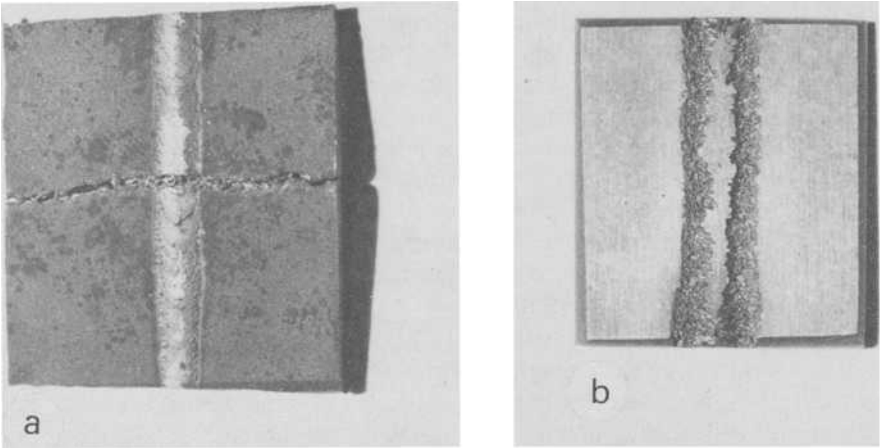

FIG. 15—*Effect of welding on* (a) *ductility and* (b) *corrosion resistance of AISI Type 446 steel; 26 percent chromium, 0.095 percent carbon, 0.077 percent nitrogen; corrosion tested in boiling ferric sulfate-50 percent sulfuric acid solution* [45].

Type 446 stainless steel after it is welded. Of all the detrimental effects which can occur in high-chromium ferritic stainless steels following heat treatment, the so-called ***high-temperature embrittlement*** is most damaging because operations such as welding, heat treatment, and casting—all operations necessary for a material of construction—can cause serious loss in ductility and corrosion resistance. Not surprisingly, this problem has been a severe deterrent, limiting extensive use of air-melted ferritic stainless for commercial construction.

Background

Exceptionally thorough survey articles by Thielsch [*6*] and Rajkay [*7*] summarize all the research done up to about 1966 on the causes for the severe loss of corrosion resistance and ductility when high-chromium steels of moderate interstitial contents are heated to high temperatures. Most early investigators studied either the embrittlement phenomenon or the corrosion loss phenomenon, although, as latter investigators showed, the property losses are related to a single mechanism. Up to the 1960's, two theories were offered to explain the severe embrittlement.

1. The segregation or coherent state theory [*6*] postulated that embrittlement resulted from a clustering or segregation of carbon atoms in the ferrite matrix. During rapid cooling, most of the dissolved carbon in solid solution does not reprecipitate as carbides. Instead, the carbon atoms in the supersaturated ferrite phase group as coherent clusters which harden (that is, embrittle) the matrix, much in the manner of certain age-hardening alloys. Annealing affected alloys between 700 and 800°C causes the carbon to precipitate as carbides, thereby removing the carbon atom clusters and the embrittlement.

2. In the martensitic mechanism first described by Pruger [*46*], regions in the alloy of relatively high-carbon content transform to austenite at elevated temperature. During subsequent cooling, these regions transform to brittle martensite. Annealing in a temperature range of 700 to 800°C removes the embrittlement by transforming the martensite to ferrite and chromium carbides.

The theories proposed up to about 1960 to explain the severe intergranular attack on high-chromium ferritic alloys following high-temperature exposure are summarized next.

1. Houdremont and Tofaute [*47*] postulated that a carbon-rich austenite forms at the sensitizing temperature. When cooled, easily dissolved iron carbides precipitate at the grain boundaries between the austenite and ferrite phases. By annealing at about 750°C, the iron carbides are converted to chromium carbides which resist chemical dissolution, and, therefore, the material becomes resistant to intergranular attack.

2. Hochmann [*44*] also proposed the need for austenite formation at temperature but suggested that intergranular corrosion occurs by preferential attack on the grain boundary austenite phase itself because of its low-chromium and high-carbon content.

3. Lula, Lena, and Kiefer [*48*] reject any mechanism of intergranular attack that requires the formation of austenite. As they pointed up, operations aimed at preventing austenite formation following high-temperature exposure did not prevent intergranular corrosion. These workers proposed that the stress surrounding the carbide or nitride precipitates formed during cooling are the cause of rapid corrosion on the matrix adjacent to the precipitates. Annealing between 650 and 815°C annealed out the stresses caused by the precipitated phases, thus restoring corrosion resistance.

An interesting point is the lack of any suggestion by the early investigators that the high-temperature loss in corrosion resistance was due to chromium depletion adjacent to chromium-carbide precipitates. This mechanism proposed by Bain et al [*49*] in 1933 and detailed by Ebling et al [*50*] has been generally accepted as the cause of intergranular attack in 18Cr-8Ni austenitic stainless steels. Application of this phenomenon to explain intergranular corrosion in a ferritic stainless steel was difficult because the effects of heat treatment on the austenitic and the ferritic stainless steel were opposite. It was known that an austenitic stainless steel would sensitize by holding in a temperature range from 400 to 800°C and that the corrosion resistance of a sensitized specimen could be restored by heating to temperatures above about 950°C which dissolved the chromium carbide precipitates. In direct contrast, an air-melted ferritic stainless steel is sensitized whenever it is heated above about 950°C. Further, the corrosion resistance of a sensitized ferritic specimen can be recovered by annealing in a temperature range from 700 to 850°C which corresponds to a part of the range where an austenitic stainless steel is sensitized. In light of these contrasting effects, attribution of the chromium depletion theory as the mechanism for corrosion loss in ferritic stainless steel did not appear possible.

High-Temperature Loss of Corrosion Resistance

In the early and mid-1960's, a renewed interest in ferritic stainless steels resulted in research studies into the mechanism for the ***high-temperature embrittlement and corrosion*** loss phenomenon. It was Baumel in 1963 [*51*] who discussed the application of the chromium depletion theory to ferritic stainless steels. In the ten years between 1960 and 1969, investigations by Bond and Lizlovs [*52*], Bond [*53*], Baerlecken et al [*2*], Demo [*45,54*], Hodge [*43,55*], and Streicher [*56*] confirmed that the chromium depletion theory is the most plausible explanation for the severe intergranular attack which occurs when alloys of moderate carbon and nitrogen content are heated above about 950°C and then cooled to room temperature. Henthorne [*57*] has compiled an extensive summary on the factors causing intergranular attack in iron- and nickel-base alloys.

Demo [*54*] showed, in 1968, curious effects of heat treatment on the corrosion resistance of a commercial AISI Type 446 stainless steel exposed to Streicher's ferric sulfate-sulfuric acid test (M. A. Streicher, ASTM Bulletin, No. A229-58, April 1958, pp. 77-86, ASTM A262-70, Part 3, and Ref *56*). In a series of tests summarized in Table 5, he showed the poor corrosion resistance of specimens water quenched or air cooled from 1100°C and the recovery when the sensitized specimens were reheated to 850°C. However, specimens which were cooled slowly in the furnace from 1100°C to temperatures below 1000°C and then quenched displayed corrosion resistance equivalent to the annealed specimen. Based on these data and metallographic examination, Demo proposed two hypotheses but favored the one describing the existence of a chromium carbide-nitride precipitation range in the temperature region from 500 to 900°C similar to that observed for an austenitic stainless steel. Bond [*53*] in 1968 described the effects of carbon and nitrogen level on the sensitization of ferritic stainless steels containing 17 percent chromium. He concluded that intergranular corrosion of ferritic stainless steel is caused by the depletion of chromium in areas adjacent to where chromium-rich carbides and nitrides precipitate. A portion of Bond's data is tabulated in Table 6 and show the effects of interstitial levels on the intergranular corrosion re-

TABLE 5—*Effects of thermal treatment on the corrosion resistance of AISI Type 446 stainless steel.*[a]

Specimen[b] Designation	Condition	Corrosion Rate.[a] mil/year (exposure h)
1	as-received	30 (120)
2	30 min, 1100°C, water quench	780 (24)
3	30 min, 1100°C, air cool	800 (24)
5	30 min, 1100°C, water quench + 30 min, 850°C, water quench	42 (120)
4	30 min, 1100°C, slow cool to:[c]	
	1000°C, water quench	767 (120)
	900°C, water quench	27 (120)
	800°C, water quench	20 (120)
	700°C, water quench	18 (120)
	600°C, water quench	25 (120)

NOTE—Data by Demo [*54*].

[a] Exposed to boiling ferric sulfate-50% sulfuric acid solution (ASTM Recommended Practice A 262-70, Part 3).

[b] See Fig. 6 for microstructure of designated specimens.

[c] 2.5°C/min in furnace.

TABLE 6—*Results of the boiling 65% nitric acid test on selected 17Cr alloys containing carbon and nitrogen.*

		Corrosion Rate, mm/dm^2 day, for the average of 5 Successive 48-h Periods After 1 h of Heat Treatment at Indicated Temperature, water quench			
Carbon, %	Nitrogen, %	1450°F (788°C)	1700°F (926°C)	1900°F (1038°C)	2100°F (1150°C)
0.0021	0.0095	167	185	148	326
0.0025	0.022	164	944	...	761
0.0044	0.057	186	...	577	357
0.012	0.0089	126	824	1817	...
0.061	0.0071	147	619	1574	...

NOTE—Data by Bond [*53*].

sistance of a series of 17Cr alloys in boiling 65 percent nitric acid. Based on these and other data, Bond concluded that a 17Cr-Fe alloy containing 0.0095 percent nitrogen and 0.0021 percent carbon was resistant to intergranular corrosion after sensitizing heat treatment in the range of 900 to 1150°C. He also pointed up that alloys containing more than 0.022 percent nitrogen and more than 0.012 percent carbon were quite susceptible to intergranular corrosion after sensitizing heat treatments at temperatures higher than about 926°C (1700°F). The low interstitial requirement for resisting sensitization needs to be emphasized in contrast to the interstitial levels of about 0.06 percent carbon and 0.03 percent nitrogen in a typical air-melted 17Cr Type 430 stainless steel. Bond also showed, through electromicroscopic examination of the alloys susceptible to intergranular corrosion, grain boundary precipitates which were absent in alloys not susceptible to such corrosion.

Demo [*45*] in 1971 showed that a 26Cr alloy containing 0.014 percent carbon and 0.004 percent nitrogen after heating to 1000°C had excellent intergranular corrosion resistance if quenched and poor resistance if air (or more slowly) cooled. These results by Bond and Demo showed that ferritic stainless steel could be subjected to high temperature without resulting loss of corrosion resistance, providing low maximum interstitial levels were maintained in the alloys, obviously much below levels for air-melted alloys. For these low interstitial ferritic alloys, the response to heat treatment is remarkably similar to that observed for austenitic chromium-nickel stainless steels. If heated above 1000°C and water quenched, the intergranular corrosion resistance is excellent, and no grain boundary precipitates of chromium carbides are observed; upon slow cooling, severe intergranular attack may be observed along with grain boundary precipitates of chromium carbides [*49,58*]. A clear relationship between heat treatment, the presence of an intergranular precipitate, and corrosion resistance exists for a low interstitial ferritic alloy.

For a commercial air-melted Type 446 (26 percent chromium) stainless steel, Demo [*45*] showed there is not a one-to-one correlation between loss of corrosion resistance and the presence of a continuous grain boundary precipitate in contrast to austenitic stainless steels and low interstitial ferritic stainless steels. These results are shown in Fig. 16 for specimens whose corrosion resistance is summarized in Table 5. For example, specimens with microstructures numbered 2 (water quenched from 1100°C) and 3 (air cooled) had poor intergranular corrosion resistance consistent with the continuous chromium-rich precipitates observed in the grain boundaries. Specimens 1 (as-received) and 4 (cooled slowly from 1100°C) showed excellent intergranular corrosion resistance consistent with the essential lack of any grain boundary precipitate. However, Specimen 5 (reheated at 850°C) showed excellent intergranular corrosion resistance but also a heavy grain boundary precipitate usually indicative of poor corrosion resistance. It is lack of correlation between corrosion resistance and grain boundary precipitate and the fact that commercial alloys become sensitized when heated above about 1000°C that have held back the acceptance of the theory that the *high-temperature sensitization* problem in ferritic stainless steel is caused by chromium-rich precipitates formed at grain boundaries when the alloys are cooled through a temperature from about 400 to 900°C.

Using selected Fe-26Cr alloys of reduced interstitial levels, Demo [*45*] defined the sensitization range for 26Cr-Fe alloys (0.1 in. thick). To do this, he used alloys which had excellent corrosion resistance when quenched from 1100°C but poor corrosion resistance if air cooled such that the quenched alloys were supersaturated in carbon and nitrogen at room temperature. The water-quenched alloys were then subjected to a second heat treatment at selected times and temperatures between 400 and 1000°C. The alloys were corrosion tested and microstructurally examined. From the corrosion data, Demo constructed a time-temperature-sensitization envelope (TTS) for 26Cr-Fe ferritic stainless steel as shown in Fig. 17. The microstructure of selected examples (whose positions are marked on Fig. 17) and their corrosion resistance are tabulated in Fig. 18. Specimen 1 heated at 1100°C and water quenched had good corrosion resistance consistent with the absence of grain boundary precipitates. Specimen 2, on the other hand, air cooled from 1100°C, had poor corrosion resistance consistent with the grain boundary precipitates of chromium-rich carbides and nitrides. Specimen 3, water quenched from 1100°C, then reheated at 900°C, had good corrosion resistance and a harmless discontinuous intergranular precipitate. Comparing micrographs of Specimens 3 to 1 offers very strong evidence that chromium-rich materials precipitate even at 900°C, followed by agglomeration and growth of the precipitates. Specimen 4, reheated for a short time at

700°C, exhibited good corrosion resistance, but the presence of a continuous intergranular precipitate is evident. At this temperature, the rapid precipitation of chromium-rich carbides and nitrides to relieve supersaturation was compensated for by almost simultaneous diffusion of chromium which healed the initial chromium-depleted areas adjacent to the precipitate. On the other hand, Specimen 5, heated for the same time as Specimen 4 but at 600°C, showed severe intergranular corrosion as well as a continuous grain boundary precipitate. Under these conditions of time and temperature, the rapid precipitation of chromium-rich precipitates occurred to relieve supersaturation; but, with reduced diffusion rates, chromium atoms did not have time to diffuse into the depleted areas. This fact is demonstrated by Specimen 6, also exposed at 600°C, but for a long time (6 h). The specimen had a continuous grain boundary precipitate, but, unlike Specimen 5, it had good corrosion resistance. The longer hold time allowed the chromium atoms to diffuse into the chromium-depleted areas adjacent to the grain boundary precipitate restoring the alloys corrosion resistance. In consideration of Fig. 17, the line marking the low temperature side of the TTS band reflects the minimum time and temperature required for chromium-rich carbides and nitrides to precipitate from a supersaturated solid solution and to form chromium-depleted zones. The line marking the high-temperature side of the sensitization zone represents for 0.1-in. material, minimum conditions of time and temperature necessary for chromium diffusion to occur and heal the depleted areas after the matrix supersaturation in interstitial levels has been relieved by precipitation of chromium-rich carbides and nitrides.

These data are consistent with the chromium depletion theory for intergranular corrosion. When ferritic stainless steels are heated above about 950°C, the chromium-rich carbide and nitride precipitates are dissolved in solid solution. If the interstitial levels are very low, they will be maintained in solid solution if the specimen is cooled rapidly. For these quenched alloy compositions, the corrosion resistance is good. If these alloys now supersaturated in carbon and nitrogen are subjected to temperatures from about 500 to 950°C, chromium-rich carbides and nitrides precipitate rapidly to relieve supersaturation. In the temperature range of about 700 to 950°C, almost as soon as precipitation occurs, chromium diffuses into the chromium-depleted areas formed when precipitation first occurred, increasing the chromium content of these areas. Consequently, intergranular corrosion resistance is good, despite the observed presence of an intergranular precipitate. In the temperature range of 500 to 700°C where chromium-rich carbides and nitrides rapidly precipitate, the resulting chromium-depleted zones are not healed except during long hold times because the diffusion rate of chromium is markedly lower at these lower temperatures.

In light of this description, the chromium depletion theory can also

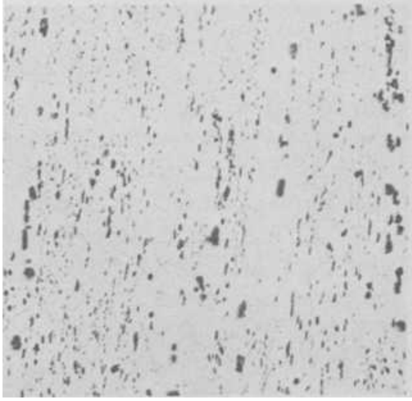

(1) AS RECEIVED

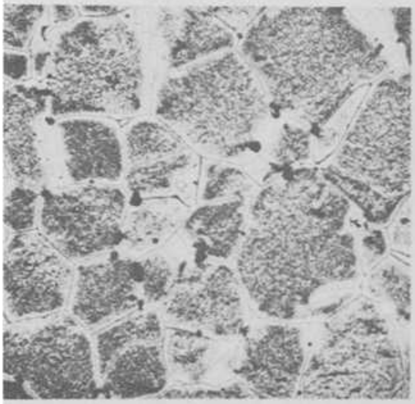

(2) 30 MIN., 1100 °C, W.Q.

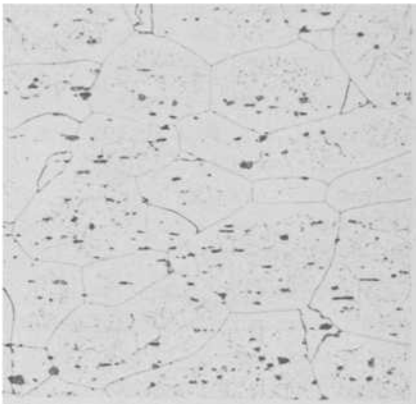

(3) 30 MIN., 1100 °C, A.C.

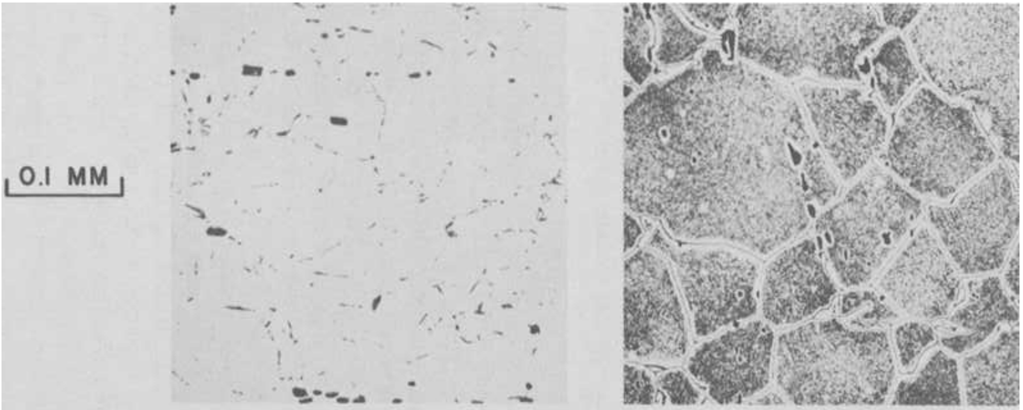

(4) 30 MIN., 1100 °C, W.Q.
+ SLOW COOL TO 850 °C, W.Q.

(5) 30 MIN., 1100 °C, W.Q.
+ 30 MIN., 850 °C, W.Q.

FIG. 16—*Relationship between thermal treatments and microstructure on an AISI Type 446 steel; 26 percent chromium, 0.095 percent carbon, 0.077 percent nitrogen; see corrosion rates for specimens in Table 5* [45].

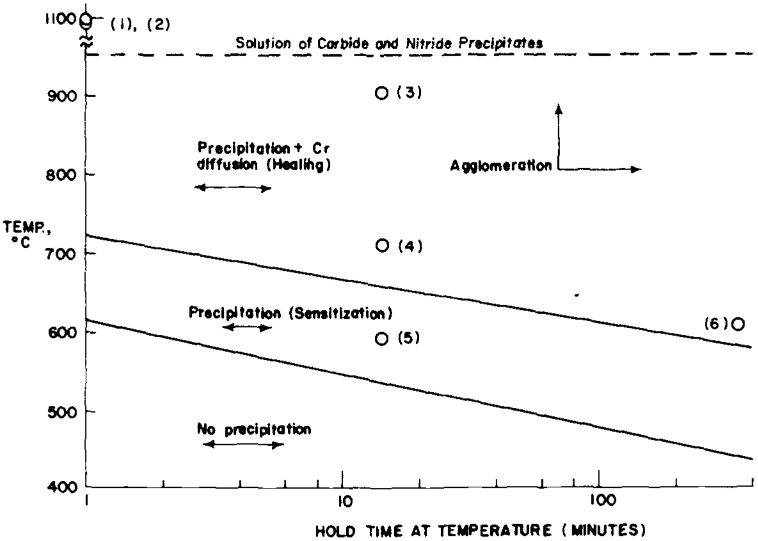

FIG. 17—*TTS diagram for Fe-26Cr alloys treated initially at 1100°C, 30 min, water quenched, then reheated at selected lower temperatures for different times; corrosion tested in boiling ferric sulfate-50 percent sulfuric acid solution; (carbon + nitrogen) ≈ 180 ppm* [45].

explain the effects of heat treatment on the corrosion resistance and microstructure on the high interstitial alloys like AISI Types 430 and 446 stainless steel. For these alloys, in contrast to the low interstitial alloys, even rapid quenching from temperatures above 950°C is not fast enough to prevent precipitation of chromium-rich carbides and nitrides and chromium depletion results. This behavior is produced by the high driving force for precipitation in the intermediate temperature ranges caused by a combination of high interstitial supersaturation, rapid diffusion of carbon and nitrogen as compared to chromium, and high rates of precipitation in the ferritic matrix. The corrosion resistance of a sensitized high interstitial alloy can also be restored by heating in the temperature range of about 700 to 950°C. This heat treatment permits chromium to diffuse into the depleted areas, raising the chromium content and restoring corrosion resistance, even though a grain boundary precipitate may still be observed in the microstructure (Specimen 5, Fig. 16). A long-time heat treatment in this temperature range, as used in commercial annealing practices, may even allow sufficient time for the fine grain boundary precipitate to agglomerate into large, discontinuous precipitates which are thermodynamically more stable and often observed for long-time heat treatments (Specimens 1 and 4, Fig. 16).

In 1970, Hodges [*43,55*] demonstrated that high-purity alloys from 17 to 26 percent chromium were highly resistant to intergranular cor-

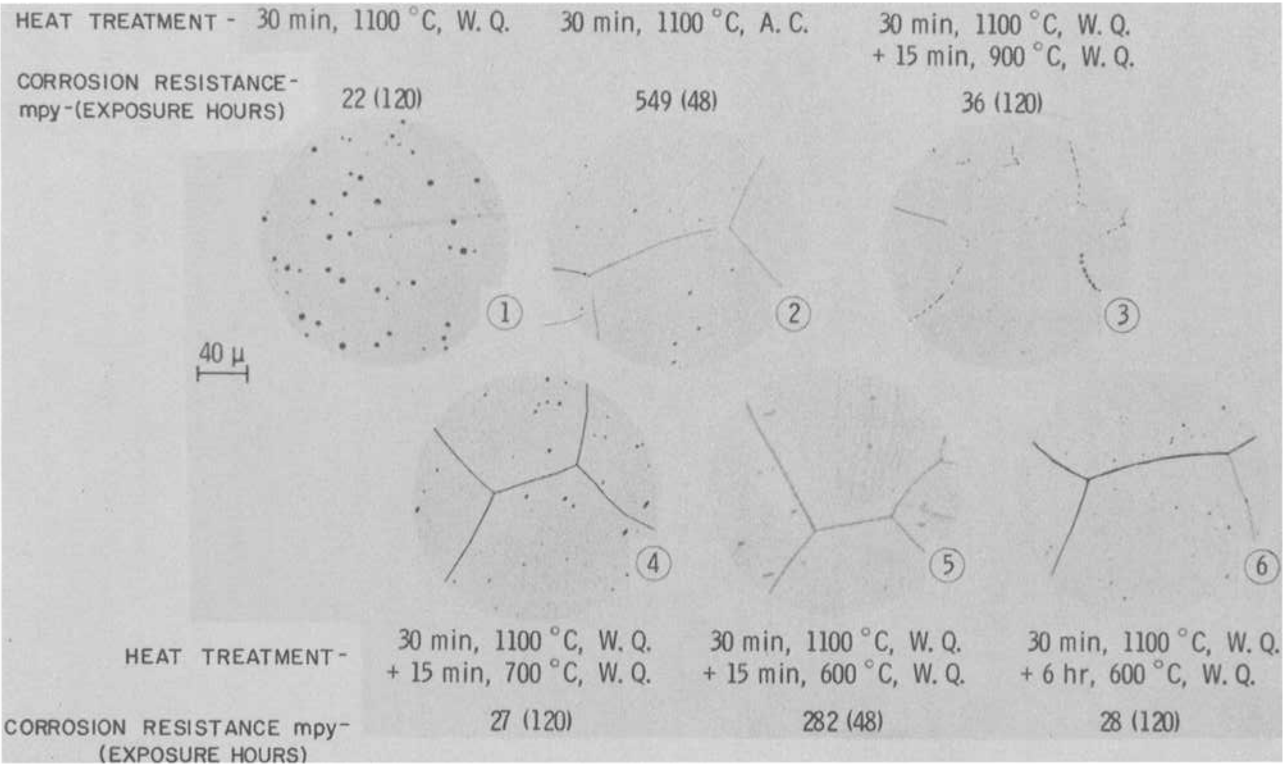

FIG. 18—*Microstructure and corrosion resistance of alloys treated as indicated by numbered positions on TTS diagram in Fig. 17; corrosion tested in boiling ferric sulfate-50 percent sulfuric acid solution* [45].

rosion following exposures to temperatures above about 950°C. Based on his work, he concluded that sensitization in ferritic stainless steels could be explained best on the basis of the chromium depletion theory. Hodges noted that the sensitization-desensitization behavior of ferritic stainless steels containing moderately low interstitial levels could be described by the same type of TTS curve as reported for austenitic stainless steels, the difference being that the time sequence for sensitization-desensitization for austenitic stainless steel is minutes and hours, but only seconds and minutes for ferritic stainless steels. Hodges also showed that molybdenum as an alloying element in high-purity ferritic stainless steels shifts the sensitizing envelope to longer times, thereby delaying sensitization and loss of intergranular corrosion resistance. Streicher [*59*] showed that, for high-purity ferritic alloys, the interstitial levels which are tolerable without sensitization occurring is increased when molybdenum additions up to 6 and preferably 4 percent are made.

Streicher [*56*] has studied in detail the effects of carbon and nitrogen level and heat treatment on the microstructure and corrosion resistance of chromium-iron alloys. In particular, he has documented carefully the regions of attack in specimens which are fully ferritic or a mixture of ferrite and austenite, depending on where the alloy composition was located according to the phase diagrams in Fig. 3 when it was exposed to high temperatures. As an example taken from his work, a commercial Type 446 steel (26 percent chromium) containing 0.098 percent carbon and 0.21 percent nitrogen contains up to about 40 percent austenite when water quenched from a heat treatment at 1150°C. As shown in Fig. 19*a* from Streicher's work, no chromium-rich precipitates of carbon and nitrogen are formed at the boundary between austenite grains or in the austenite grains themselves because of the high solubility of carbon and nitrogen in austenite. When this specimen was subjected to the ferric sulfate-sulfuric acid corrosion test, (Fig. 19*b*), severe intergranular attack occurred at the ferrite-ferrite and ferrite-austenite boundaries because carbon and nitrogen were rejected due to the low interstitial solubility in ferrite. However, no attack is observed at the austenite-austenite boundaries because the interstitials are maintained in solid solution due to their high solubility in austenite. Streicher [*56*] also showed that heat treatments have no detrimental effects on the intergranular corrosion susceptibility of high-purity 16 and 25Cr-Fe stainless steels (carbon $\leqslant$ 0.0086 percent, nitrogen $\leqslant$ 0.0025 percent). From his work, he also concludes that the chromium depletion theory can adequately explain intergranular corrosion and other forms of localized attack occurring in chromium-iron stainless steels.

Based on the work of a number of investigators, the *high-temperature loss of corrosion resistance* observed when ferritic alloys of high interstitial contents are heated above about 950°C may be explained by

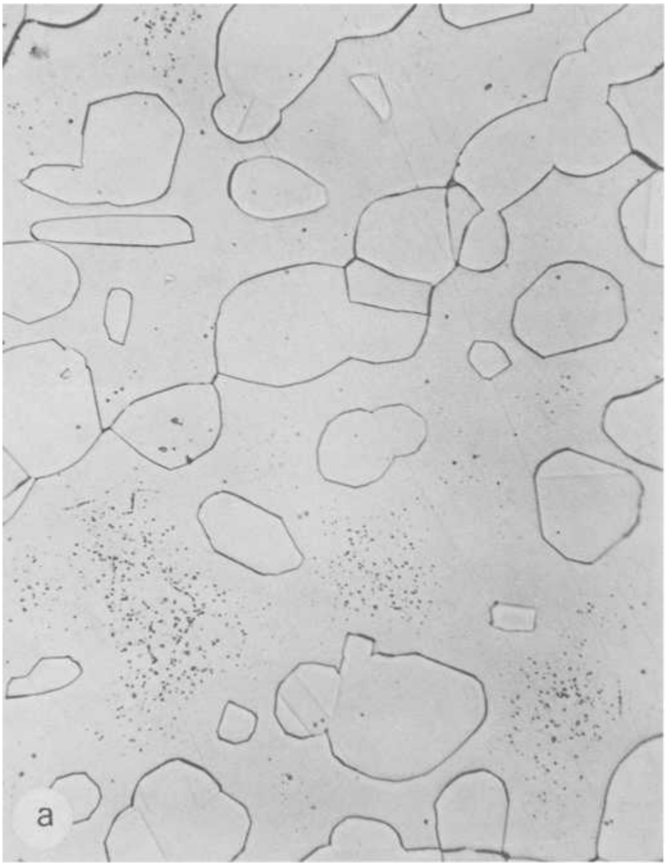

FIG. 19*a—Structure of Type 446 steel heated at 1150°C (×500). Etched surface shows "dot" precipitate in ferric matrix, but not near austenite grains, which have absorbed carbon and nitrogen from adjacent ferrite.*

the chromium depletion theory which is accepted widely as the cause for sensitization in austenitic stainless steels. No support for alternate theories proposed to explain the *high-temperature corrosion loss* phenomenon can be found. These alternate theories were based on (*a*) preferential dissolution of iron carbides, (*b*) accelerated corrosion due to stresses surrounding chromium rich precipitates, (*c*) presence of austenite or its decomposition products at grain boundaries, and (*d*) galvanic action between the precipitate and the surrounding metal matrix.

High-Temperature Embrittlement

Whenever commercial high chromium-iron ferritic stainless steels con-

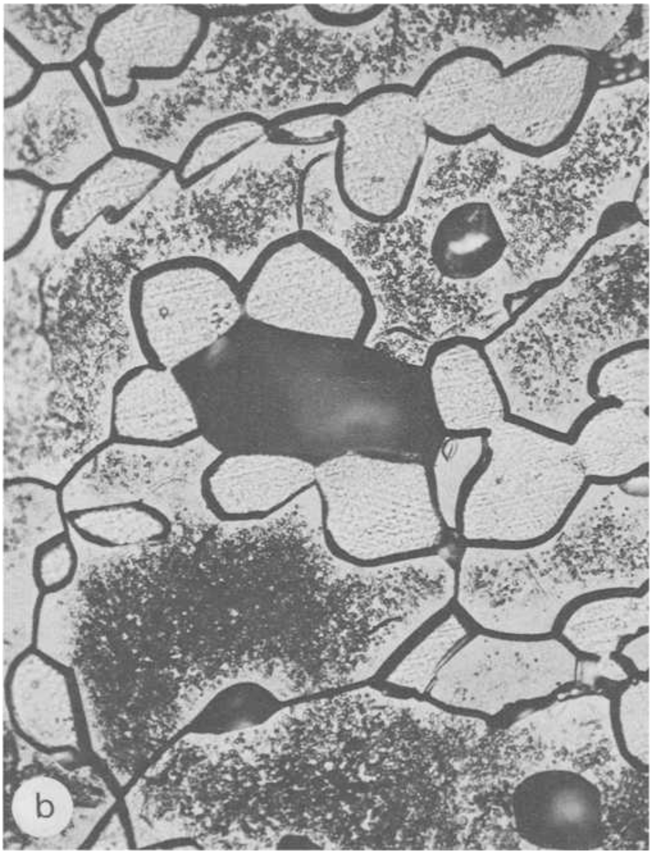

FIG. 19*b—Initial attack of ferric sulfate solution on Type 446 steel heated at 1150°C, water quenched (×500). Intergranular attack on ferrite-ferrite and ferrite-austentite boundaries. No intergranular attack on austenite-austenite boundaries. Localized attack on dot precipitates which are absent in zones near austenite grains but not at ferrite-ferrite boundaries; exposed 14 h in boiling ferric sulfate-50 percent sulfuric acid solution* [56].

taining moderate to high interstitial levels are heated above about 1000°C, the alloys at room temperature show an extreme loss in toughness and ductility. If an embrittled alloy is reheated in a temperature range of 750 to 850°C, the ductility of the alloy is restored. Two early theories, coherent state and the martensitic mechanism, proposed to explain this high-temperature embrittling phenomenon were described earlier. Baerlacken et al [*2*], Demo [*45*], Semchyshen et al [*60*], and Plumtree et al [*61*] have shown through their work that *high-temperature embrittlement* is related to interstitial levels in the alloy just as is loss of intergranular corrosion resistance.

Baerlecken et al [2] studied the effects of heat treatment on the toughness (impact strength) of air-melted steels containing moderate levels of carbon and nitrogen and vacuum-melted steel containing very low interstitial levels. Using air-melted steel, these workers concluded that the variable toughness as a function of heat treatment and chromium content was connected with the structure and morphology of the carbide precipitates. Using high-purity, vacuum-melted alloys given a two-stage heat treatment (30 min at 1050°C cooled to 800°C for 25 h) these workers showed that the impact transition temperature was shifted to higher temperatures as the chromium content increased. However, if these same low interstitial alloys were given a second high-temperature heat treatment by reheating to 1050°C which would normally embrittle a high interstitial alloy, they discovered that excellent low-temperature impact values were observed for alloys at all chromium levels. These results are shown in Fig. 20 from their work. They explained this effect of heat treatment on toughness by the fact that the solubility of the interstitials in the α solid solution decreases with increasing chromium content. There-

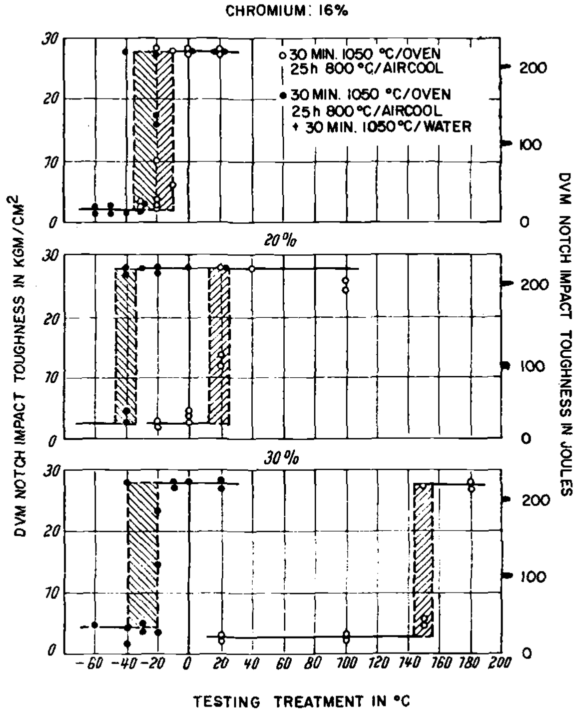

FIG. 20—*Effect of heat treatment on position of the sharp drop of the notch impact toughness-temperature curve of vacuum-melted chromium steels with 16 to 30 percent chromium* [2].

fore, the initial two-stage heat treatment on specimens of the same interstitial levels produces more precipitates of carbides and nitrides the higher the chromium content of the alloy is, with resulting decrease in toughness (that is, increase in the transition temperature). On the other hand, by a second solution heat treatment and rapid quenching, it is possible even with steels of high-chromium content (and reduced carbon and nitrogen solubility) to keep the very low interstitial levels of vacuum-melted alloys in solid solution. Therefore, carbides and nitrides do not precipitate, and their deleterious effects on notch impact toughness do not occur. Another important conclusion from their work is that grain size has little effect on notch impact behavior because high-chromium, vacuum-melted alloys even with grain size ASTM 1-3 displayed transformation temperature of about −40°C.

Demo [*45*] studied the effect of thermal treatment on the ductility of high and low interstitial purity alloys containing 26 percent chromium. As shown in Table 7, loss of ductility is observed only when the commercial

TABLE 7—*Effect of thermal treatments on the ductility of stainless alloys.*

Condition	Elongation (in 25.4 mm) for the Indicated Stainless Steels After Heat Treatment: AISI Type 446	High Purity[a] 26Cr	AISI Type 304
Annealed	25	30	78
30 min, 1100°C, water quench	2	30	84
30 min, 1100°C, air cool	27	32	85
30 min, 1100°C, slow cool[b] to 850°C, water quench	33	30	. . .
30 min, 1100°C, water quench + 30 min, 850°C, water quench	27	29	. . .
120 min, 677°C, air cool[c]	. . .	. . .	84

NOTE—Data by Demo [*45*].

[a] 0.014% carbon, 0.004% nitrogen.

[b] Cooled in furnace at 2.5°C/min.

[c] A heat treatment known to cause sensitization in AISI Type 304.

AISI Type 446 stainless steel containing high interstitial levels is heated to 1100°C and water quenched. Importantly, the same alloy cooled more slowly from the high-temperature exposure (that is, air or slow cooled) shows excellent ductility, as does the embrittled alloy when it is annealed by a second heat treatment at 850°C. In contrast, the ductility of the low interstitial 26 percent chromium steel is not adversely affected by heat treatment. These observations suggested to Demo that loss of ductility (that is, tensile elongation) in chromium-iron alloys when heated to high temperature, as in welding or isothermal heat treatment, was also related to interstitial content, as suggested by Baerlacken et al, and cooling rate. Demo also examined the fractured edges of the heat-treated, air-melted Type 446 stainless steels in cross section, as shown in Fig. 21. The water-quenched specimen (brittle) shows intragranular cleavage. The air-cooled specimen (ductile) shows intergranular cleavage with some localized deformation and elongation of the grains. The slowly cooled specimen (ductile) shows a fibrous shear structure with considerable localized deformation and elongation of the grains. Based on these observations, Demo concluded that precipitation of carbides and nitrides in the grain boundaries does not grossly affect ductility because both air-cooled and water-quenched specimens had intergranular precipitates, but the failure mode in the brittle specimen was predominantly intragranular. Moreover, an embrittled specimen reheated to 850 °C shows restored ductility despite the presence of a heavy intergranular precipitate, as shown in Fig. 16 (Specimen 5). Finally, as shown in Table 7, an 18Cr-8Ni austenitic stainless steel, which has been sensitized by heating at 677 °C to cause grain boundary precipitation of chromium carbides, retains excellent ductility.

Using thin-film electron microscopy examination, Demo has shown structural difference between embrittled and ductile alloys. Transmission micrographs of the water-quenched specimen (brittle) and the air-cooled specimen (ductile) are shown in Fig. 22. For the water-quenched specimens, precipitates are noted, not only in the grain boundaries as expected from the optical micrographs, but also on nearly all dislocations. On the other hand, no precipitates are observed on the dislocations of the air-cooled specimens, although grain boundary precipitation is shown in the optical micrograph. Unrestrained motion of the dislocations in the water-quenched specimen is blocked by the precipitate, with a resulting increase in strength and reduction in ductility and toughness.

Demo proposed that precipitation of chromium-rich carbides and nitrides on dislocations in the grain body and not on grain boundary surfaces is responsible for the severe loss in ductility when ferritic alloys are heated to high temperature. Demo suggests two possibilities to explain why chromium-rich precipitates form on dislocations in rapidly cooled specimens and not on more slowly cooled specimens, even though both contain chromium-rich precipitates in the grain boundaries. First, the high interstitial contents of the air-melted alloys, combined with the high interstitial supersaturation, serves as a strong driving force during quenching for rapid precipitation on all high-energy surfaces such as grain boundaries and dislocations. During a slower cool, the longer relative time available to relieve supersaturation may allow for diffusion of carbon and nitrogen to grain boundary areas where the supersaturation is relieved by precipitation on the more preferred higher energy surfaces of the grain boundary. An alternate explanation is that dislocation nucleation during the rapid quench occurs simultaneously with rejection of carbon and nitrogen as

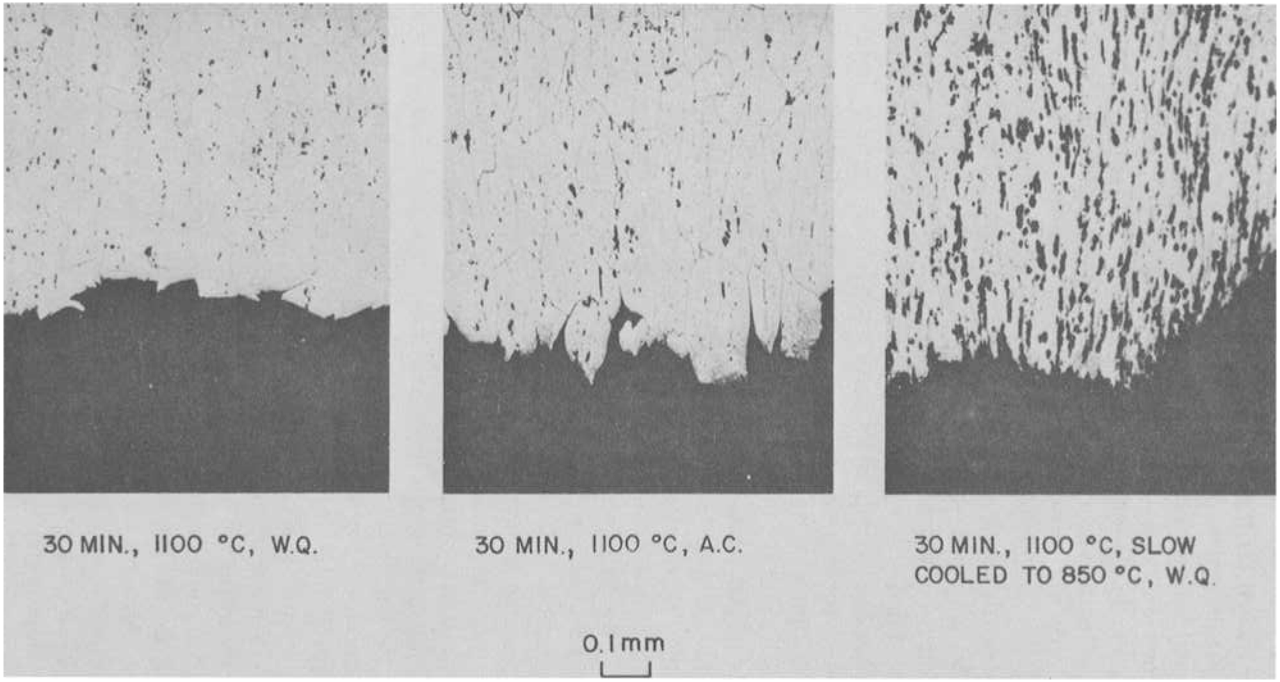

FIG. 21—*Effect of cooling rate on morphology of the fracture edges of a tension specimen made of an AISI Type 446 stainless steel heated to 1100°C; 0.095 percent carbon, 0.077 percent nitrogen. Furnace slow cool ~2.5°C/min* [45].

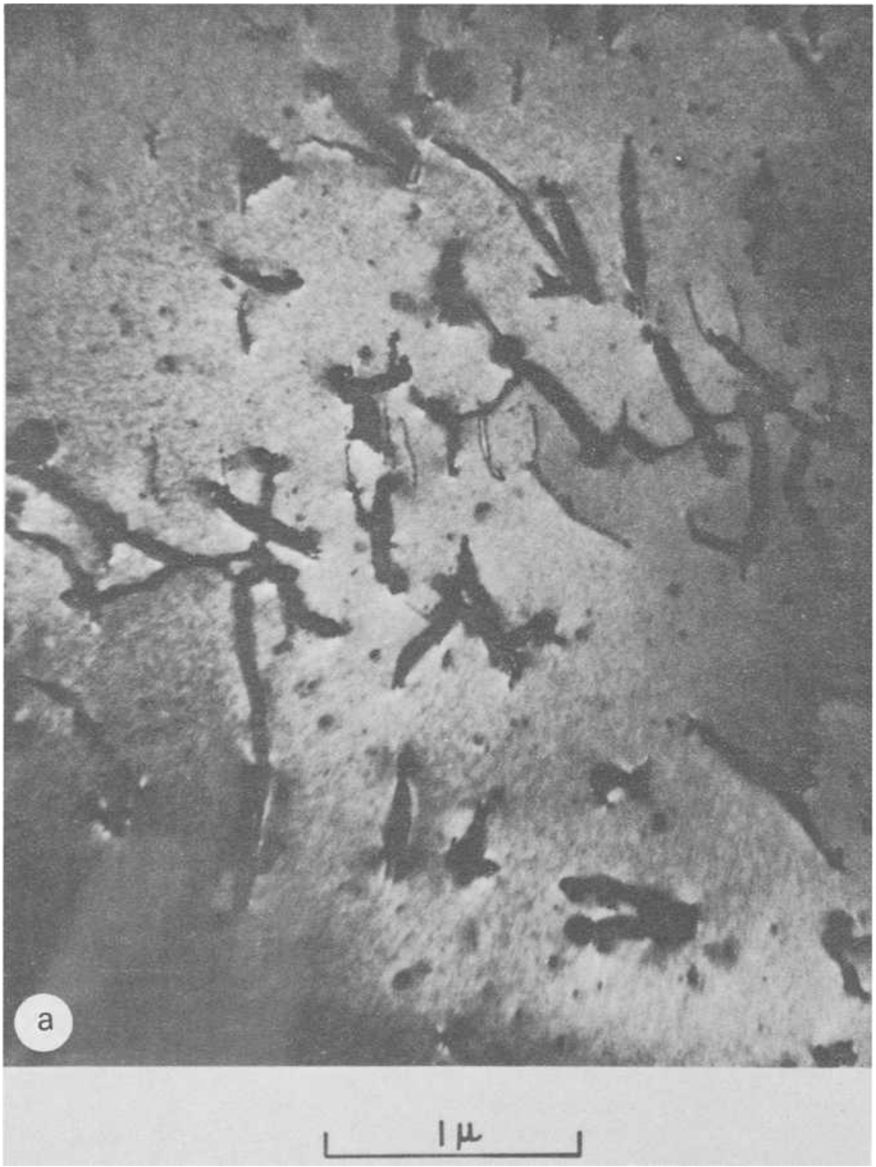

(*a*) Water quenched.

FIG. 22—*Transmission electron micrographs of an AISI Type 446 stainless steel heated to 1100°C; 0.095 percent carbon, 0.077 percent nitrogen* [54].

(*b*) Air cooled.

FIG. 22—*Continued.*

chromium-rich carbides and nitrides precipitate to relieve the supersaturation. With a slower cool and, therefore, reduced thermal stresses, relief of supersaturation by precipitation on high-energy surfaces may occur before dislocations are nucleated by the effects of thermal stresses. Demo associates the poor ductility of chromium-iron alloys subjected to high-temperature exposure to fine, dispersed precipitates in the matrix preventing easy movement of dislocation similar to a hardening mechanism in a precipitation-hardened alloy [*62*]. An increase in strength is observed with a concomitant tremendous reduction in ductility and toughness.

Semchyshen, Bond, and Dundas [*60*] have reported the effects of chromium, carbon, and nitrogen levels and heat treatment on the toughness (impact resistance) of chromium-iron alloys containing from about 14 to 28 percent chromium. The impact resistance of a 17Cr steel in the annealed condition as a function of carbon content is shown in Fig. 23*a*. Note the relatively low transition temperatures even at carbon levels of 0.061 percent. These data may be contrasted with impact energy absorbed for the same specimens sensitized by heating to 1150°C as shown in Fig. 23*b*. When the carbon content of the alloys exceeds about 0.018 percent carbon, a large increase in transition temperature is observed. As noted, these alloys contain low levels of nitrogen ($<$0.0010 percent). These same workers repeated this work on a series of alloys containing increasing levels of nitrogen, with carbon being held to low levels below 0.004 percent. The impact data for the annealed specimens and those annealed, as well as heated at 1150°C are shown respectively in Figs. 24*a,b*. The annealed specimens containing nitrogen up to 0.057 percent displayed excellent impact resistance. However, when the nitrogen content in the 17Cr alloys exceeded about 0.022 percent nitrogen, the impact transition temperature was shifted to high temperatures following a thermal treatment at 1150°C. The same effects between carbon, nitrogen, heat treatment, and impact resistance were found for alloys containing 26 percent chromium. Semchyshen et al also showed that a 17Cr alloy containing 0.01 percent carbon or 0.02 percent nitrogen contained grain-boundary precipitates, while alloys of higher purity remained free of grain boundary precipitate after quenching from temperatures above about 925°C. Based on these data and observations, they conclude that *high-temperature embrittlement* (that is, the observed increase in transition temperature when ferritic alloys are quenched from temperatures above about 1000°C) is caused by precipitates of chromium-rich carbonitrides mainly on the grain boundaries.

Plumtree et al [*61*] showed in recent work that the impact transition temperature increased linearly with the total interstitial content for 25Cr-Fe alloys annealed and water quenched. The data show a change in transition temperature from below room temperature to above in the range from 350 to 450 ppm total carbon plus nitrogen plus oxygen. These workers also showed that the impact transition temperature increases with the second

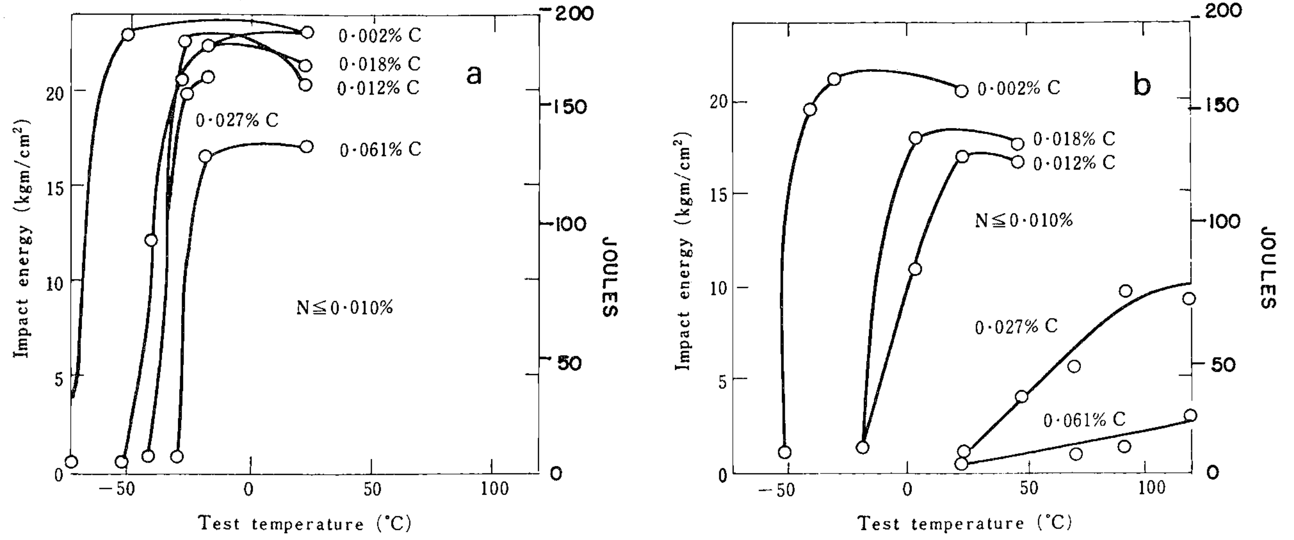

FIG. 23—*Transition curves for quarter-size Charpy V-notch impact specimens of 17Cr-0.002 to 0.61C. Ferritic stainless steels heat treated at*: (a) *815°C for 1 h and water quenched or* (b) *815 + 1150°C for 1 h and water quenched* [60].

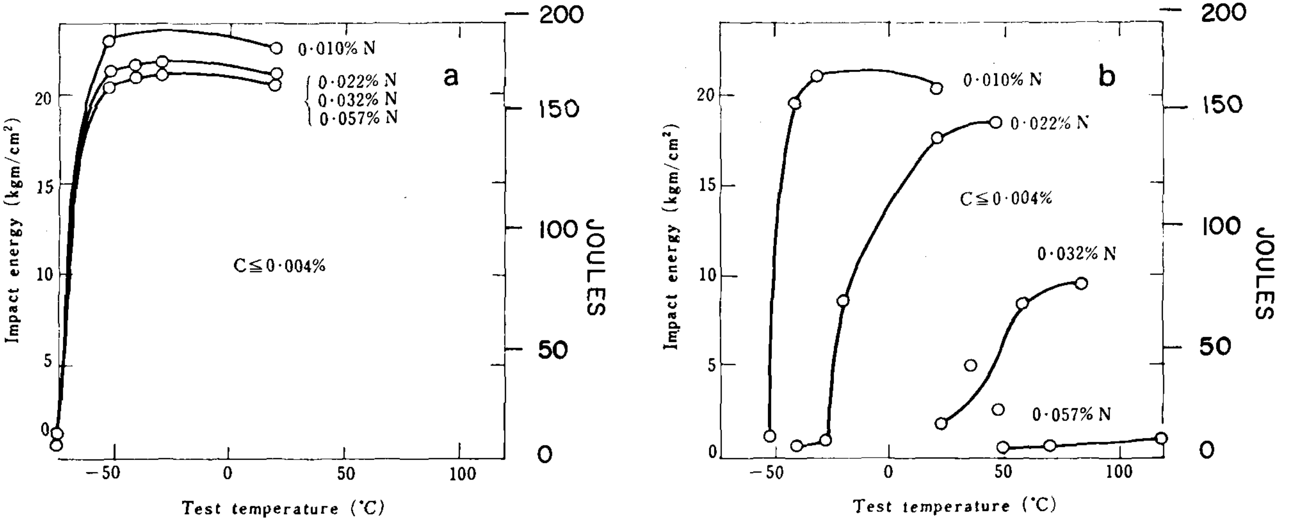

FIG. 24—*Transition curves for quarter-size Charpy V-notch impact specimens of 17Cr-0.010 to 0.057N ferritic stainless steels heat treated at*: (a) *815°C for 1 h and water quenched or* (b) *815 + 1150°C for 1 h and water quenched* [60].

phase content, and they proposed that increasing amounts of second phase inhomogeneously distributed throughout the matrix, particularly at the grain boundaries, lower the effective surface energy of a crack to promote cleavage failure and brittleness.

Baerlecken et al [*2*], Demo [*54*], Semchyshen et al [*60*], and Plumtree et al [*61*] all conclude from their data that the so-called ***high-temperature embrittlement*** phenomenon of high-chromium ferritic stainless steels is due to precipitation of chromium-rich carbides and nitrides caused by relief of supersaturation when the alloys are exposed to high temperatures. Baerlacken et al and Semchyshen et al find the embrittlement occurs because the chromium-rich precipitate forms on grain boundaries, while Demo and Plumtree claim the embrittlement occurs because a finely dispersed precipitate in the grain matrix hinders dislocation motion, and precipitates in the grain boundaries do not necessarily indicate alloy embrittlement. Perhaps the difference in thought resides in testing severity. A grain boundary precipitate may be detrimental to the high-rate energy absorbing requirement of the impact test but perhaps not detrimental to the slow-rate energy absorbing requirement of the tensile or slow bend test. The important point, however, is the general agreement that the ***high-temperature embrittlement*** phenomenon observed in ferritic stainless steels is dependent upon the levels of carbon and nitrogen in the alloys. The embrittlement problem in chromium-iron alloys will manifest itself whenever alloys containing moderate or high interstitial levels are heated to temperatures above about 950°C. The embrittlement is caused by precipitation of chromium-rich carbides and nitrides on grain boundaries or dislocations or both. It is at once apparent that the same precipitation mechanism causing embrittlement also produces the serious loss of corrosion resistance when ferritic alloys are heated to high temperatures.

Notch Sensitivity in Annealed Alloys

Unlike the austenitic stainless steels, annealed chromium-iron stainless steels are highly notch sensitive in a manner similar to mild and low alloy steels [*25,63,64*]. In 1935, Krivobok [*65*] showed that the room-temperature impact resistance of chromium-iron alloys in the presence of a notch declined sharply when the chromium content exceeded about 15 percent, and this decline in properties was independent of carbon content in the range of 0.01 to 0.20 percent. These data are shown in Fig. 25. Heger [*66*] did a comprehensive study of the effects of notching on the tensile and impact strength of annealed air-melted 27Cr-Fe alloys measured at room temperature and at elevated temperatures. These data were reported by Newell in 1946 [*24*]. Looking first at the effect of a notch on tensile properties, Heger showed that the tensile strength increased and the elongation decreased in the presence of a notch. These effects are shown in Fig. 26 for

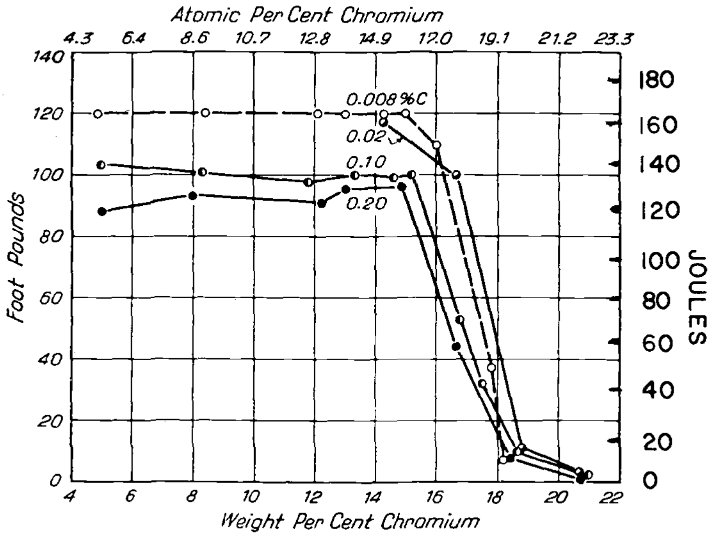

FIG. 25—*Effect of variation in chromium and carbon content on notch impact toughness of commercial chromium stainless steels* [65].

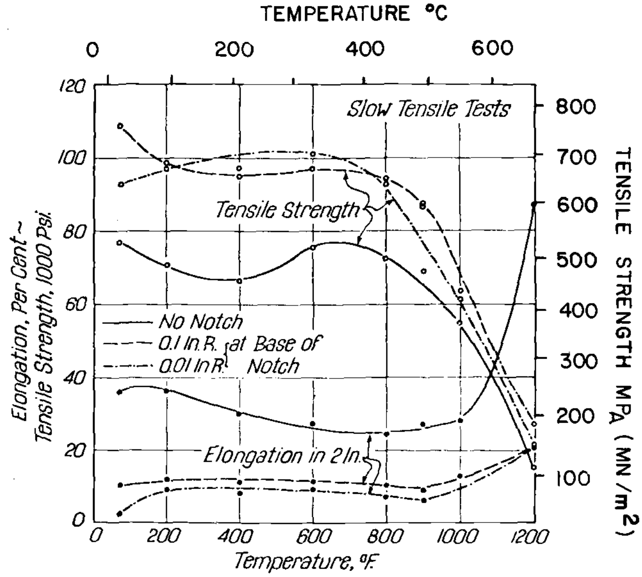

FIG. 26—*Effect of a notch on the short-time, high-temperature tensile properties of 27Cr-Fe air-melted alloy* [25,66].

short time tests run from room to elevated temperature. The difference in tensile and elongation properties between notched and unnotched specimens remained, even up to temperatures of 426 to 538°C. When Heger considered the effect of a notch on the impact resistance of a 27Cr-Fe alloy, he found a surprising difference in the impact energy absorbed between the notched and unnotched specimens. Similar to Krivobok's data, the notched specimen showed low impact energy absorption, but the unnotched specimen had high impact energy absorption. These data from Heger's work are shown in Fig. 27 along with the effect of testing temperature. There is a wide difference in the energy absorbed between the unnotched and notched specimen at room temperature which persists up to about 870°C testing temperature. However, the magnitude of the difference in impact absorption energy between the two types of specimens decreases as temperature increases because the impact absorption energy for the unnotched specimen declines and increases for the notched specimen. At temperatures of 870°C and above, the alloy was no longer notch sensitive. These data indicate the value of preheating air-melted chromium-iron alloys to reduce notch sensitivity in severe forming operations.

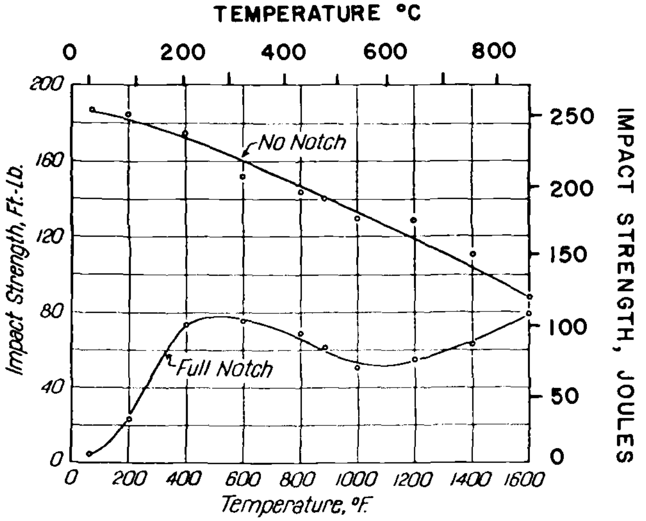

FIG. 27—*Effect of temperature on impact properties of 27Cr-Fe, air-melted alloy. No notch versus full notch* [25,66].

Based on data from Krivobok and Heger, it was generally believed into the late 1940's that notch sensitivity occurred independent of carbon and nitrogen content [*63,67*] and, in fact, was associated with the high-chromium content of the alloys *per se*. Later work by Hochmann [*68*] and Binder and Spendelow [*69*] showed that notch sensitivity in annealed chromium-iron alloys with high-chromium levels was again basically caused by the presence of critical levels of interstitial elements, particularly carbon, nitrogen, and oxygen. The dramatic effects of interstitial level on the impact behavior of annealed chromium-iron alloys were discovered when vacuum melting techniques were developed and used to produce alloys with extremely low interstitial levels.

The impact strength measured at room temperature of vacuum-melted chromium-iron alloys as a function of chromium content is shown in Fig. 28 from Binder et al [*69*]. The maximum interstitial content of the alloys

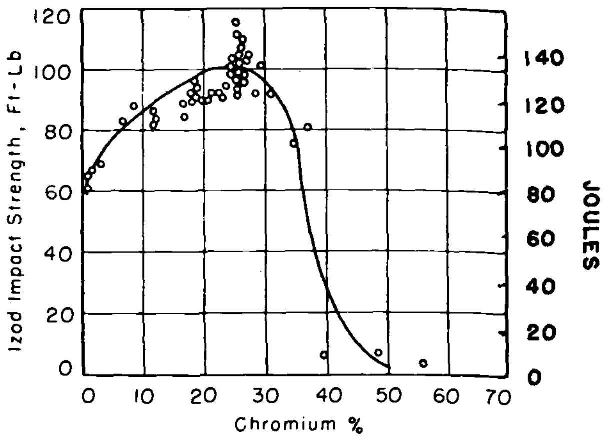

FIG. 28—*Impact strength of vacuum-melted chromium-iron alloys* [69].

used to generate these data include carbon 0.015 percent, nitrogen 0.01 percent, and oxygen 0.04 percent. As shown in Fig. 28, the toughness of these high-purity alloys increases as chromium content is raised, reaching a maximum at about 26 percent chromium, where unheard-of impact strength values of 100 ft·lb (136 J) are apparent. In contrast to Krivobok's data, [*65*] (Fig. 25) which showed a sharp drop in impact strength for alloys containing more than about 16 percent chromium, use of the vacuum melting process has raised the level of chromium, for which excellent impact toughness may be obtained in the presence of a notch from 16 percent to somewhat greater than 35 percent. The key to this difference in impact performance between normal air-melted steels and vacuum-melted alloys is primarily in their carbon and nitrogen content. The relationship between interstitial content and chromium content on toughness was determined in a very comprehensive investigation by Binder and Spendelow [*69*], as shown in Fig. 29. At chromium levels above about 15 to 18 percent, there is a drastic decrease in the carbon and nitrogen levels tolerable in a high-chromium alloy for high room-temperature impact resistance. For an air-melted steel with carbon and nitrogen contents up to about

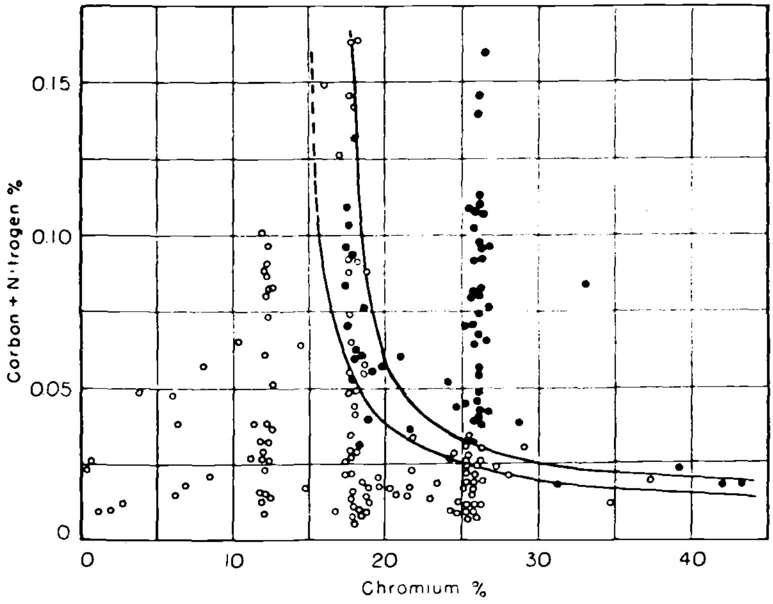

FIG. 29—*Influence of carbon and nitrogen on toughness of chromium-iron alloys. Open circles: high-impact strength alloys; solid circles: low-impact strength alloys* [69].

0.12 and 0.05 percent [*69*], respectively, these data would predict good room-temperature impact resistance is possible only if the alloys contain chromium levels below 15 to 18 percent. The agreement with Krivobok's early data [*65*] on air-melted alloys is excellent, but the conclusion that poor impact resistance was due to chromium content *per se* was incorrect. The low impact resistance of Krivobok's alloys containing more than 15 to 18 percent chromium was not caused by the chromium level but was due to the high interstitial levels characteristic of air-melted steels.

Binder and Spendelow, in their comprehensive investigation, also determined the individual effects of carbon and nitrogen on impact resistance of annealed alloys at two levels of chromium, 18 and 25 percent. These data are tabulated in Figs. 30 and 31, respectively. Both figures show: (*a*) that a straight line of a 45-deg slope may be drawn to separate the areas of high and low toughness, (*b*) that there is an equivalency in the effect by carbon and nitrogen on toughness, (*c*) that the carbon plus nitrogen sum is critical rather than the absolute value of each separately, and (*d*) that the maximum sum of carbon plus nitrogen tolerable for good room-temperature toughness is 0.055 percent for 18 percent chromium and 0.035 percent for 25 percent chromium.

Until the late 1960's, achieving levels of 0.035 percent and lower was possible only in the laboratory. With the development of economical vacuum melting and vacuum and gas refining techniques, commercial

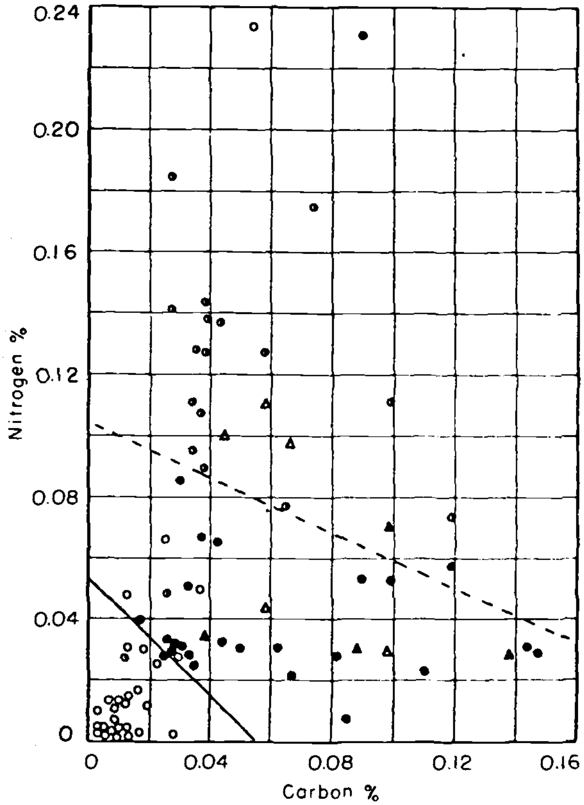

FIG. 30—*Effects of carbon and nitrogen on toughness of 17 to 19Cr-Fe alloys. Open circles: high-impact strength alloys; solid circles: low-impact strength alloys; semi-solid circles: intermediate impact strength alloys; triangles represent commercial arc-melted steels* [69].

production of high chromium-iron alloys became feasible and a reality. These alloys, to be described later, show excellent toughness at room temperature in the presence of notches. However, for available air-melted alloys such as AISI Type 430 (18 percent chromium), Type 442 (20 percent chromium), and Type 446 (26 percent chromium), notch sensitivity is a factor of major importance which must be considered carefully in application of these alloys. Good engineering practices require avoiding surface scratches and reentrant angles, notches, or other forms of stress risers when these air-melted alloys are used under shock loading conditions.

Weldable, Corrosion-Resistant, Ductile Ferritic Stainless Steels

The largest single drawback to the use of ferritic stainless steels has been the loss of corrosion resistance and ductility following exposures to high temperatures, as in welding and isothermal heat treatments. The

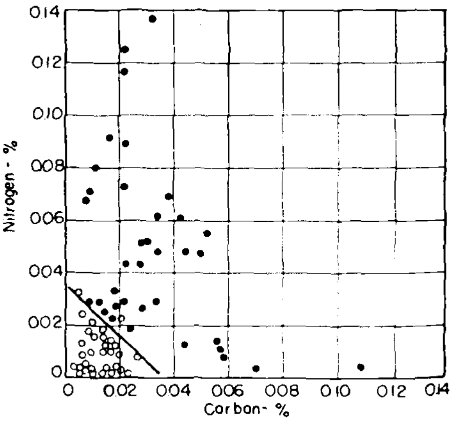

FIG. 31—*Effects of carbon and nitrogen on toughness of 24 to 26Cr-Fe alloys. Open circles: high-impact strength alloys; solid circles: low-impact strength alloys* [69].

other problems with ferritic stainless steel (475°C and σ-phase embrittlements) can be tolerated because relatively long exposure times at moderate temperatures are required to cause these other embrittling problems. However, unless a material has good corrosion resistance and ductility in the as-welded condition, its usefulness as a material of construction is limited severely. As just described, the cause for the serious loss in ductility and corrosion resistance when ferritic stainless steels are exposed to high temperatures and for the notch sensitivity of annealed alloys is related to the interstitial content of the alloys. After research in the early and mid-1960's had shown this fact, the research effort in the late 1960's saw development and commercialization of weldable, corrosion-resistant chromium-iron alloys. To reach this position, three routes to achieve interstitial control were researched and developed. Demo [*70*] has summarized and described these methods used to achieve interstitial controls in ferritic stainless steels.

Low Interstitials

By reducing the interstitial levels below certain minimum values, weldable and corrosion resistance can be produced, as shown in the works of Hochmann [*68*], Demo [*70*], Bond [*53*], Streicher [*56*], and Hodges [*43,55*]. Binder's [*69*] (Fig. 29) early work showed how the impact resistance of annealed ferritic stainless steels varied with interstitial and chromium content. A similar type of study by Demo [*70*] showed the relationship of interstitial level and chromium content on the ductility and corrosion resistance of as-welded alloys. These data are summarized in Fig. 32 and include a comparison to Binder's data for impact resistance on annealed specimens. The carbon and nitrogen levels which can be present in an alloy without affecting the weldability of a chromium-iron alloy are low and decrease rapidly with increasing chromium content. As can be seen from the data in Fig. 32, the interstitial tolerance level for a "good" as-welded specimen at a given chromium level is lower than that needed for impact resistance of an annealed specimen. Demo further studied the variation in the properties of weld ductility and weld corrosion resistance as functions of chromium content and interstitial sum level. These data are tabulated in Table 8. As chromium content increases from 19 to 35 percent, the amount of carbon plus nitrogen that can be tolerated for intergranular corrosion resistance increases somewhat. Conversely, for as-welded ductility, the sum of tolerable interstitials is reduced drastically.

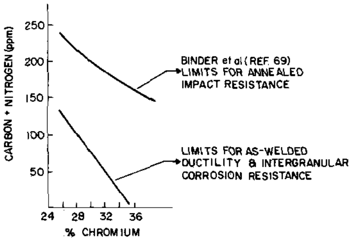

FIG. 32—*Effects of carbon and nitrogen level and chromium content on as-welded ductility and intergranular corrosion resistance of chromium-iron ferritic stainless steels. Comparison to Binder's limit for impact resistance of annealed specimens* [70].

TABLE 8—*Carbon plus nitrogen limits for as-welded properties of intergranular corrosion resistance and ductility as a function of chromium content.*

	Limit for Sum of C + N (ppm) to Have the Indicated Property in an As-Welded Alloy[a]	
Chromium Level, % by weight	Intergranular[b] Corrosion Resistance	Ductility[c]
19	60 to 80	>700
26	100 to 130	200 to 500
30	130 to 200	80 to 100
35	~250	<20

NOTE—Data by Demo [*70*].

[a] Sample thickness: 0.1 in. (2.54 mm) thick.

[b] Intergranular corrosion resistance in boiling ferric sulfate-50% sulfuric acid solution.

[c] No cracks, as determined by bending around a 0.2-in. mandrel.

At low chromium levels, as-welded corrosion resistance is the factor controlling whether an alloy has good weldability; at high-chromium levels, as-welded ductility is the limiting factor. At the 26 percent chromium level, intergranular corrosion resistance is more sensitive to the interstitial sum level than is ductility while at 35 percent chromium; the as-welded ductility is more critically dependent on the interstitial sum than is corrosion resistance.

To produce weldable and corrosion-resistant chromium-iron alloys by this route, it is evident that very low levels of carbon and nitrogen are needed. Until recently, such low levels could only be produced in a laboratory or by using high-purity raw materials. However, technological advances in steel-making practices have made the concept of low interstitial ferritic alloys possible through the development of such techniques as oxygen-argon melting, vacuum refining, and electron-beam refining. Of particular note is the electron-beam continuous hearth refining technique developed by Airco Vacuum Metals and described by Knoth [*71*]. This process has the advantage of achieving the lowest carbon and nitrogen levels by exposing a high surface to volume ratio of molten metal to a high vacuum for extended periods of time. As the molten metal flows down a series of water-cooled copper hearths, electron beam heat sources provide localized regions of intense heat in the molten metal, causing volatilization and removal of tramp impurity elements. The process is being used currently to produce commercially a high-purity ferritic stainless steel containing nominally 26 percent chromium, 1 percent molybdenum, and balance iron. By maintaining the carbon plus nitrogen level below 250 ppm, it is reported [*72,73*] that this commercially available alloy is ductile and corrosion resistant following welding, has good toughness, and combines resistance to stress-corrosion cracking with good general corrosion and pitting resistance. However, for a weldment to be resistant to intergranular attack, a carbon plus nitrogen sum level at or near 250 ppm is too high. Demo [*45*] reports intergranular attack on a high-purity 26Cr alloy containing 180-ppm carbon plus nitrogen, while Streicher [*59*] (Table 2) shows grain dropping in the weld and heat-affected zone of two high-purity 26Cr-1Mo alloys containing 105 and 230-ppm carbon plus nitrogen, respectively. For complete resistance to intergranular attack following welding or isothermal heat treatment, it appears that the carbon plus nitrogen levels in 26Cr and 26Cr-1Mo high-purity alloy systems must be maintained below about 100 to 120 ppm [*70*] with nitrogen [*59*] less than 90 ppm. The high-impact values at and below room temperature for an electron beam refined 26Cr-1Mo alloy as compared to a 26Cr-1Mo alloy containing 0.08 percent carbon is remarkable, as shown in Fig. 33 [*60, 72*]. The scatterband in the E-Brite 26-1 alloy data is the result of specimen orientation, variations in thermal treatments, and cooling rates.

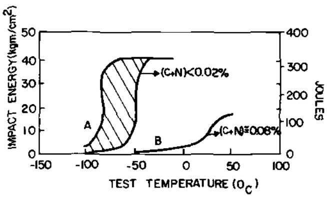

FIG. 33—(a) *Charpy V-notch transition temperature range for commercially produced electron-beam-melted ferritic steel containing 26 percent chromium and 1 percent molybdenum* (*E-Brite 26-1*) [72]. (b) *Transition curve for quarter-size V-notch impact specimens of an air-melted steel containing 26 percent chromium and 1 percent molybdenum* [60].

Interstitial Stabilization

A second means to control interstitials is to add elements to the alloy which form stronger carbides and nitrides than does chromium. Such elements include titanium, columbium, zirconium, and tantalum. The early work by Lula, Lena, and Kiefer [*48*] describes a comprehensive effort to study the intergranular corrosion behavior of ferritic stainless steel, including the effects of titanium and columbium additions. These investigators showed that titanium and columbium additions were not completely effective in preventing sensitization when the alloys were subjected to high temperature. This result was caused by not considering the need to tie up nitrogen as well as carbon and also by the unknown fact at the time that titanium carbide itself is dissolved in highly oxidizing solutions such as the boiling nitric acid solution used in the study.

More recent work by Baumel [*74*], Bond and Lizlovs [*52*], and Demo [*75,76*] have shown that columbium and titanium additions were effective in preventing intergranular corrosion following exposure of ferritic stainless steels to high temperatures such as isothermal heat treatments and welding. To resist intergranular corrosion, titanium additions of about six to ten times the combined carbon and nitrogen level are necessary; for columbium, additions of eight to eleven times are required. The relationship of interstitial content, chromium level, and titanium level for intergranular corrosion resistance and ductility after welding has been studied extensively by Demo [*75,76*]. Bond et al [*52*], Lula et al [*48*], Herbsleb [*77*], Baumel [*74*], and Cowling et al [*78*] have shown that titanium-stabilized alloys may show intergranular attack when exposed to a highly oxidizing solution such as boiling nitric acid due to dissolution of titanium carbonitrides; however, columbium-stabilized alloys resist intergranular attack even in highly oxidizing solutions.

Demo [*75,76*], Semchyshen et al [*60*], Wright [*79*], and Pollard [*80*] have reported the effects of stabilizing additions on the weld ductility of ferritic stainless steels. By introducing titanium or columbium in the ferritic alloy, the level of interstitial which can be present in the matrix without adversely affecting the room-temperature ductility after welding is increased significantly. These data are shown in Table 9 by the tensile ductility measurements on welded 18Cr-2Mo specimens [*60*] and in Table 10 by the slow bend tests on welded 26 to 30Cr alloys [*75,76,79*]. With stabilizer additions, the interstitial elements are effectively tied up as stable carbides and nitrides such that their effective level in solid solution is reduced. Consequently, stabilized alloys at relatively high levels of carbon and nitrogen act similarly to the very low interstitial alloys just described in having excellent corrosion resistance and ductility (tensile or bend) following exposure to high temperatures which, without stabilization, would cause loss of corrosion resistance and ductility.

TABLE 9—*Effect of stabilizer additions on the tensile ductility of annealed versus welded specimens containing 18% chromium-2% molybdenum.*

C + N, % by weight	Ti or Cb, % by weight	Elongation in 50 mm, % Annealed	Elongation in 50 mm, % As Welded
0.005	0	33	31
0.03	0	31	8
0.07	0.5	34	30
0.06	0.6	28	21

NOTE—Data by Semchyshen et al [*60*].

TABLE 10—*Effect of titanium on the as-welded bend ductility for chromium-iron ferritic stainless steels containing 26 to 30% chromium.*

C + N, ppm	Ti, % by weight	Bend Test Ductility As-Welded
113	0	passed 180 deg, 2t[a]
310	0	passed 180 deg, 1/2t[b]
362	0	failed 90 deg, 2t[a]
450	0	failed 90 deg, 2t[a]
900	0	failed 135 deg, 1t[b]
300	0.22	passed 180 deg, 1/2t[a]
387	0.24	passed 180 deg, 2t[a]
488	0.47	passed 180 deg, 2t[a]
850	0.45	passed 180 deg, 1/2t[b]

[a] Data by Demo [*75,76*], 0.1-in.-thick specimens. t = specimen thickness.
[b] Data by Wright [*79*], 0.06-in.-thick specimens.

The effects of stabilizing additions on the impact properties of chromium iron alloys in comparison to the impact properties of low interstitial alloys, however, presents another story. The effects of stabilizing additives on impact properties have been studied and described by Semchyshen et al

[*60*] and Wright [*79*]. Two aspects have been studied, namely, the effect of titanium content and interstitial level on the impact resistance of (*a*) annealed specimens and (*b*) specimens heated to high temperatures by welding or isothermal heat treatments. In the annealed condition, the titanium-modified steels exhibit transition temperatures commensurate with their interstitial levels; that is, whatever the impact transition temperature is for the unstabilized, annealed alloy as a function of interstitial level (see Fig. 29), remains about the same or is slightly reduced when the alloy is stabilized.

Stabilizing additions of titanium, however, are useful in reducing the detrimental effects of high-temperature treatments on the impact resistance of high interstitial alloys. These effects of stabilizing additions taken from Semchyshen et al [*60*] are shown in Fig. 34 for air-melted commercial purity (0.07 percent carbon plus nitrogen) 18Cr-2Mo alloy. Increases in titanium content from 0 to 0.8 percent show little effect on the impact transition temperature of annealed (815°C) specimens. However, increases in titanium content from 0 up to about 0.5 percent improve (lower) the transition temperature when the alloys are subjected to a high-tempera-

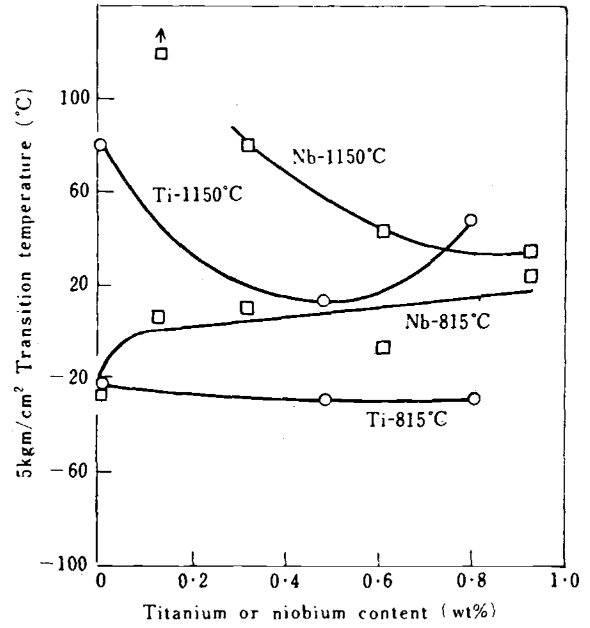

FIG. 34—*Transition temperatures for quarter-size Charpy V-notch specimens air-melted commercial-purity 18Cr-2Mo steels water quenched from 1150°C (sensitized) and 815°C (annealed) as a function of titanium or columbium content* [60].

ture treatment (1150 °C). These data also show that columbium additions, though effective in lowering the transition temperature for alloys subjected to a high temperature, were somewhat harmful to the impact resistance of the alloys in the annealed condition. Semchyshen et al [*60*] also showed that titanium additions beyond about ten times the combined carbon and nitrogen content could affect (increase) the impact transition temperature of annealed 18Cr-2Mo alloys (0.07 percent carbon plus nitrogen) as shown in Fig. 35. A precipitation of an intermetallic phase markedly increased impact transition temperatures.

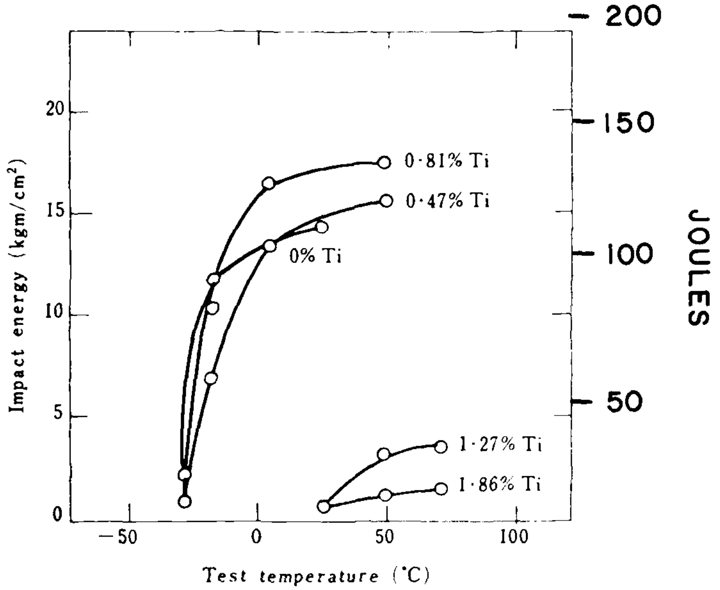

FIG. 35—*Transition curves for quarter-size Charpy V-notch impact specimens of air-melted 18Cr-2Mo; 0 to 1.86Ti ferritic stainless steels heat treated at 815 °C for 1 h and water quenched* [60].

Superimposed on the effects of titanium and interstitial content on the ductility and impact resistance of chromium-iron alloys is the marked effect of thickness on these properties, particularly impact resistance. This point is shown by the data in Table 11 taken from Wright's work [*79*]. In order to have acceptable properties (weldability and touchness) at plate gages as heavy as 0.5 in., interstitial sum level in a 26Cr alloy must be as low as or lower than about 100 to 125 ppm. For alloys containing about 300 to 900 ppm total carbon and nitrogen, toughness may be poor at gages above about 0.13 in., and weldability is poor at all gage thicknesses. The addition of titanium increases the thickness or gage level at which

TABLE 11—*Impact transition temperatures as a function of gage and added titanium for annealed 26Cr-1Mo alloys.*

	Gage Thickness, in. (mm)		
	Charpy V-Notch, Ductile to Brittle Temperature, °C		
C + N, % by weight	0.5 (12.7)[a]	0.12 to 0.14 (3.05 to 3.56)[a]	0.06 (1.52)[b]
0.0065	−57	...	−73
0.0310	149	38	−73
0.0900	162	38	−18
0.0300 + 0.22 Ti	121	−1	−46
0.0850 + 0.45 Ti	107	38	−46

NOTE—Data by Wright [79].

[a] Water quenched after anneal.

[b] Air cooled after anneal.

an alloy will have good weldability. For example, as Wright notes, a 26Cr-1Mo alloy containing 300 ppm total carbon and nitrogen and 0.22 percent titanium, has excellent toughness and weldability (that is, as-welded ductility and corrosion resistance) up to a gage thickness of about 0.13 in.

In summary, adding a stabilizer to an alloy of moderate carbon and nitrogen will not improve the annealed impact behavior significantly but may improve the as-welded ductility and corrosion resistance tremendously. This point is a most important difference between stabilized alloys and low interstitial alloys. The high-purity material will have excellent toughness and as-welded corrosion resistance and ductility. The stabilized material will also have excellent as-welded corrosion resistance and ductility but may not have high room-temperature impact resistance. These effects as shown by Wright [*79*] are particularly magnified at section thicknesses greater than about ⅛ in. Therefore, for thick plate sections where high room-temperature toughness is an absolute requirement, the low interstitial alloys would be acceptable, but the stabilized grades would not. On the other hand, for thin material, as required in heat exchanger tubing, the titanium stabilized alloys and the low interstitial alloys have similar toughness and weldability properties so that either alloy system may be used.

Weld Ductilizing Additions

A third method which produces high chromium-iron ferritic stainless steels with good as-welded ductility is to add low concentrations of selected elements with atomic radius within 15 percent of the α matrix. This method was developed and investigated extensively by Steigerwald et al [*81*]. As noted in Fig. 32, the carbon and nitrogen level for as-welded ductility is reduced drastically as chromium content increases. At 35 percent chromium, an impossibly low interstitial level of about 10 to 15 ppm is necessary for as-welded ductility. Steigerwald et al found that, in the presence of low amounts of copper, aluminum, vanadium, and combinations of these elements, alloys with good as-welded ductility could be produced at high interstitial levels. A summary of this work is shown in Fig. 36. With selective additives, an alloy containing 35 percent chromium can be produced with both as-welded ductility and corrosion resistance at interstitial levels of 250 ppm versus the 10 to 15 ppm level needed at this chromium level when the additives are absent. It is remarkable that a ferritic stainless steel containing 35 percent chromium can be made with as-welded ductility at intermediate interstitial levels.

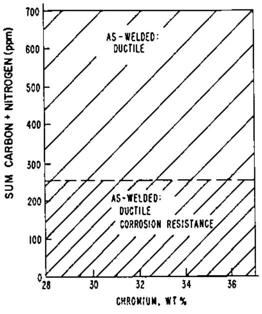

FIG. 36—*Effect of weld ductilizing additives on as-welded ductility and corrosion resistance of high chromium-iron stainless steels; additives, singly or in combination, include aluminum, copper, vanadium, platinum, palladium, and silver in a range 0.1 to 1.3 percent* [81].

Sigma Phase and 475°C Embrittlement Susceptibility

By the techniques of interstitial control, chromium-iron alloys can be produced which resist the damaging loss of corrosion resistance and ductility following high-temperature exposures, as in welding or isothermal heat treatments. In addition, some alloys can be produced to also have high room-temperature impact toughness in thick sections. Therefore, by interstitial control methods, the *high temperature* exposure and notch sensitivity problems which have limited severely the usefulness of ferritic stainless steels before have been removed. However, though not as serious as the embrittling problems described earlier, the 475°C and σ-phase embrittling phenomenon will still occur in alloy composition made resistant to high-temperature exposure effects. This point has been shown by works of Grobner [*42*], Hochmann [*44*], and in reported data for E-Brite 26-1 [*72*].

Molybdenum Additions

For improving the general corrosion and pitting resistance of chromium-iron stainless steels, the effects of molybdenum additions have been extensively studied and reported on by Bond [*82*], Demo [*70*], Streicher [*59*], and Steigerwald [*83-85*]. Of particular note here is the effect of molybdenum additions on embrittling a chromium-iron stainless steel. Semchyshen et al [*60*] have summarized the data describing the effect molybdenum level has on the toughness of 18 and 25Cr alloys. The effects of molybdenum level on the impact transition temperature of an annealed 25Cr alloy containing high and low interstitials, respectively, are shown in Fig. 37. There is considerable difference in the impact transition temperature of the high-purity alloys (−50°C) and the high interstitial alloys (+50°C) without molybdenum addition, as described earlier. The point, however, is that molybdenum additions up to about 2 to 3 percent have little effect on toughness but an adverse effect when the molybdenum level exceeds about 3 to 4 percent. This decrease in toughness associated with high-molybdenum contents is caused by the formation of chi (χ) phase, a brittle intermetallic compound of iron, chromium, and molybdenum.

Streicher [*86*] has reported on a study of the effects of heat treatment on the microstructure and formation of χ and σ phase in two low interstitial alloys containing 28 percent chromium-4 percent molybdenum and 28 percent chromium-4 percent molybdenum-2 percent nickel. One-hour heat treatment in the range of 700 to 925°C produced only a small amount of σ at the grain boundaries. The largest amounts of σ are formed by heating at 815°C. Heating for 100 h at 815°C caused σ and large amounts of χ phase to form a grain boundaries and within the grains. The complex relationship between chromium, molybdenum, and iron levels on the formation of χ and σ phases has been described in detail by the work of McMullen et al [*87*]. The ternary phase diagram for the iron-chromium-molybdenum system at 898°C (1650°F) isotherm, as defined by McMullen et al, is shown in Fig. 38 [*87*]. χ phase is stable over a wider temperature range than σ [*87*], so annealing above 980°C is required to eliminate it in steels with 18 percent chromium and over 3.5 percent molybdenum [*60*] and in steels containing 28 percent chromium-4 percent molybdenum [*86*].

For 26Cr alloys containing 1 percent molybdenum and stabilized with titanium, Aggen [*88*] and Demo [*89*] have shown that a corrosion-damaging second phase occurs in the alloy when a slight excess of titanium beyond that needed to tie up the interstitials is present. This phase, believed also to be χ, is richer than the matrix in titanium, molybdenum, and silicon and forms by isothermal holds for extended periods in the temperature range from 595 to 850°C. Before it has grown large enough to be seen by an optical microscope, the intergranular corrosion resistance

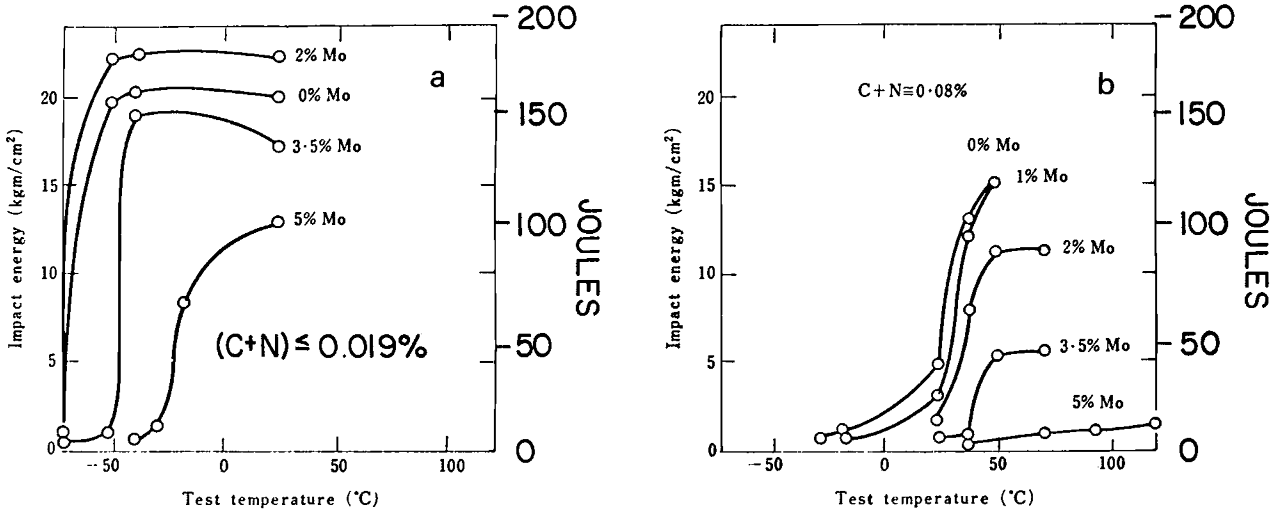

FIG. 37—*Effects of molybdenum additions on impact transition temperatures of annealed 25Cr-Fe stainless steels*: (a) *vacuum-melted stainless steels heat treated at 980°C for 1 h and water quenched or* (b) *air-melted stainless steels heat treated at 815°C for 1 h and water quenched. Quarter-size Charpy V-notch impact specimens* [60].

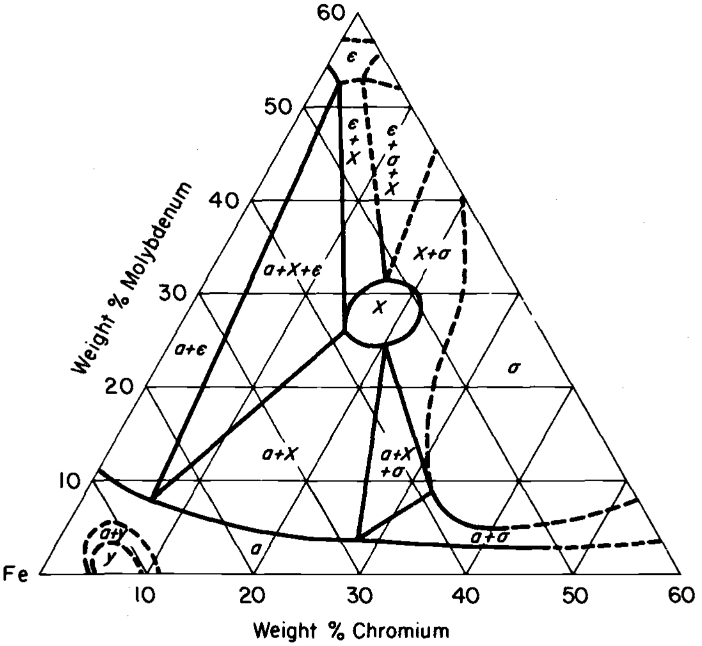

FIG. 38—*Constitution of iron-chromium-molybdenum alloys at 898°C (1650°F). σ = sigma; χ = chi; and ε = Fe_7Mo_6* [87].

of a susceptible alloy will be affected deleteriously when it is exposed to highly oxidizing solutions. The effect only appears in alloys containing molybdenum and excess titanium and can be removed by short annealing treatments at temperatures above about 900°C.

Summary

Chromium-iron alloys are bcc up to the melting point. Therefore, hardening by the ferrite-austenite mechanism upon heating and quenching cannot occur. Ferritic chromium iron alloys can be embrittled by the phenomenon of 475°C embrittlement, σ-phase embrittlement or χ-phase embrittlement for those alloys containing molybdenum. These embrittling mechanisms generally require a long-time isothermal treatment or very slow cool through the intermediate temperature regions such that they do not normally constitute a threat to the weldability and processing of ferritic stainless steels. The serious loss of ductility and corrosion resistance when ferritic stainless steels are subjected to high-temperature exposures as in welding or isothermal treatment and the problem of notch sensitivity have been shown to be related to interstitial levels in the alloys. By development of interstitial control techniques, it is now possible to produce high-chromium ferritic stainless steels which are corrosion resistant and ductile following a high-temperature exposure, as in welding or an isothermal heat treatment. Further, depending on the interstitial levels, high chromium-iron alloys can be produced, having excellent toughness and impact transition temperatures below room temperature. By making chromium-iron stainless steels weldable and tough, and combining this property with stress-corrosion resistance and good general corrosion resistance, attractive new materials of construction are and will be available to compete with austenitic 18Cr-8Ni-type stainless steels.

Several organizations throughout the world are engaged in commercial development of ferritic stainless steels. An 18Cr-2Mo alloy stabilized with columbium or titanium is being produced in Europe. A comprehensive review article on the properties of 18Cr-type ferritic alloys has been published by Schmidt and Jarleborg [*90*]. Where greater corrosion resistance is desired, several new compositions are either in commercial production or are being actively developed. These include a 26Cr-1Mo alloy produced either with extremely low interstitial levels by electron-beam melting techniques or with moderate interstitial levels stabilized with titanium and, to a lesser extent, with columbium. In commercial development are low interstitial alloys of the composition 26 percent chromium-2 percent molybdenum, 21 percent chromium-3 percent molybdenum, 28 percent chromium-2 percent molybdenum, 28 percent chromium-4 percent molybdenum, 28 percent chromium-4 percent molybdenum-2 percent nickel. These alloys have better general corrosion resistance than Type 316 stainless steel. Those like the 28Cr-4Mo and 28Cr-4Mo-2Ni alloys have been shown by Streicher [*59*] to have corrosion resistance in a variety of aggressive environments comparable or better than the highly alloyed nickel-based alloys. The complex relationship between chromium and molybdenum content on pitting resistance, ductility, and weld ductility, as studied by Streicher [*59*] is shown in Fig. 39. As shown by

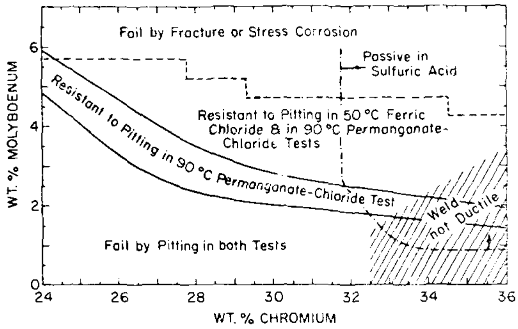

FIG. 39—*Properties of iron-chromium-molybdenum alloys. Pitting tests: 10% FeCl·6H$_2$O at 50°C (with crevices), 2 percent potassium manganate-2 percent sodium chloride at 90°C. Stress corrosion test: 45 percent boiling (155°C) magnesium chloride on welded U-bend specimens. Sulfuric acid: boiling 10 percent by weight. Carbon: 10 ppm; nitrogen: 200 ppm; carbon plus nitrogen: 250 ppm* [59].

these data, the 28Cr-4Mo-type alloys have better resistance to pitting than any other types of chromium-molybdenum-iron alloys now under development. With a variety of desirable properties available, including good weldability and resistance to stress-corrosion cracking, a family of ferritic stainless steel compositions is becoming available as materials of construction which will replace the austenitic and nickel-based alloys in many applications.

References

[*1*] Bain, E. C. and Aborn, R. H. in *Metals Handbook,* 1948 ed., American Society for Metals, p. 1194.

[*2*] Lecken, E. B., Fischer, W. A., and Lorenz, K., *Stahl und Eisen,* Vol. 81, No. 12, 1961, pp. 768–778.

[*3*] Colombier, L. and Hochmann, J., *Stainless and Heat-Resisting Steels,* Edward Arnolds Ltd. Publishers, England, 1967.

[*4*] Nehrenberg, A. E. and Lillys, P., *Transactions,* American Society for Metals, No. 46, 1954, pp. 1177–1213.

[*5*] Newell, H. D., *Metal Progress,* April 1947, pp. 617–626.

[*6*] Thielsch, H., *Welding Journal,* Research Supplement, Vol. 30, 1951, pp. 209s–250s.

[*7*] Rajkay, L., *Proceedings,* American Society for Testing and Materials, Vol. 67, 1967, pp. 158–169.

[*8*] Kaltenhauser, R. H., *Metals Engineering Quarterly,* Vol. 11, May 1971, pp. 41–47.

[*9*] Demo, J. J. and Bond, A. P., *Corrosion,* Jan. 1975.

[*10*] Cook, A. J. and Jones, F. W., *Journal of the Iron and Steel Institute,* No. 148, 1943, pp. 217–223.

[*11*] Chevenard, P., *Travaux et Memoires Du Bureau International Des Poids et Mesures,* Vol. 17, 1927, p. 90.

[*12*] Bain, E. C. and Griffiths, W. E., *Transactions of the American Institute of Mining and Metallurgical Engineers,* Vol. 75, 1927, pp. 166–213.

[*13*] Anderson, A. G. H. and Jette, E. R., *Transactions,* American Society for Metals, Vol. 24, 1936, pp. 375–419.

[*14*] Jette, E. R. and Foote, F., *Metals and Alloys,* Vol. 7, 1936, pp. 207–210.

[*15*] Smith, G. V., *Iron Age,* Vol. 166, No. 22, 1950, pp. 63–68; No. 23, 1950, pp. 127–132.

[*16*] Duwez, P. and Baen, S. R. in *Symposium on the Nature, Occurrence, and Effects of Sigma Phase, ASTM STP 110,* American Society for Testing and Materials, 1951, pp. 48–54.

[*17*] Menezes, L., Roros, J. K., and Read, T. A. in *Symposium on the Nature, Occurrence, and Effects of Sigma Phase, ASTM STP 110,* American Society for Testing and Materials, 1951, pp. 71–74.

[*18*] Dickens, G. J., Douglas, A. M. B., and Taylor, W. H., *Nature,* No. 167, 1951, p. 192.

[*19*] Heger, J. J., *Metal Progress,* Vol. 49, 1946, p. 976B.

[*20*] Shortsleeve, F. J. and Nicholson, M. E., *Transactions,* American Society for Metals, Vol. 43, 1951, pp. 142–156.

[*21*] Olzak, Z. E., "The Effect of Alloy Composition on Sigma Phase Precipitation in 27% Chromium-Iron Catalyst Tubes, First Step Dehydogenation, Plains Plant," Report No. PR-4-2, The Babcock and Wilcox Tube Co., 25 Aug. 1944.

[*22*] Heger, J. J. in *Symposium on the Nature, Occurrence, and Effects of Sigma Phase, ASTM STP 110,* American Society for Testing and Materials, 1951, pp. 75–78.

[*23*] Gilman, J. J., *Transactions,* American Society for Metals, 1951, pp. 101–187.

[*24*] Zapffe, C. A. and Worden, C. O., *Welding Journal,* Research Supplement, Vol. 30, 1951, pp. 47s–54s.

[*25*] Newell, H. D., *Metal Progress,* May 1946, pp. 977–1028.

[*26*] Zapffe, C. A., Worden, C. O., and Phebus, R. L., *Stahl und Eisen,* Vol. 71, 1951, pp. 109–119.

[*27*] Becket, F. M., *Transactions,* American Institute of Mining, Metallurgy, and Petroleum Engineers, No. 131, 1938, pp. 15–36.

[*28*] Riedrich, G. and Loib, F., *Archiv fur das Eisenhuttenwesen,* Vol. 15, No. 7, 1941-1942, pp. 175-182.

[*29*] Bandel, G. and Tofaute, W., *Archiv fur das Eisenhuttenwesen,* Vol. 15, No. 7, 1941-1942, pp. 307-319, (Brutcher Translation No. 1893).

[*30*] Heger, J. J., *Metal Progress,* Aug. 1951, pp. 55-61.

[*31*] Thielsch, H., *Welding Journal,* Research Supplement, Vol. 29, 1950, pp. 126s-132s.

[*32*] Houdremont, E., *Hanbuch der Sonderstahlkune,* Springer Verlag, Berlin, Germany, 1943.

[*33*] Masumoto, H., Saito, H., and Sugihara, M., *Scientific Reports of Tohoku University,* Series A, Vol. 5, 1953, p. 203.

[*34*] Pomey, G. and Bastien, P., *Revue de Metallurgie,* Vol. 53, 1956, pp. 147-160.

[*35*] Takeda, S. and Nagai, N., *Memoirs of the Faculty of Engineering,* Nagoya University, Vol. 8, 1956, p. 1.

[*36*] Shull, C. G., Wollan, E. O., Koehler, W. C., and Strauser, W. A., American Engineering Council Publication, ORNL-728, Oak Ridge National Laboratory, 1950.

[*37*] Williams, R. O., *Transactions,* Metallurgical Society of the American Institute of Mining, Metallurgical, and Petroleum Engineers, No. 212, 1958, pp. 497-502.

[*38*] Tisinai, G. F. and Samans, C. H., *Journal of Metals,* Oct. 1957, pp. 1221-1226.

[*39*] Fisher, R. M., Dulis, E. J., and Carroll, K. G., *Transactions,* American Institute of Mining, Metallurgical, and Petroleum Engineers, No. 185, 1957, pp. 358-374.

[*40*] Williams, R. O. and Patton, H. W., *Journal of the Iron and Steel Institute,* No. 185, 1957, pp. 358-374.

[*41*] Marcinkowski, M. J., Fisher, R. M., and Szirmae, A., *Transactions,* American Institute of Mining, Metallurgical, and Petroleum Engineers, 1964, pp. 676-689.

[*42*] Grobner, P. J., *Metallurgical Transactions,* Vol. 4, 1973, pp. 251-260.

[*43*] Hodges, R. J., *Corrosion,* Vol. 27, 1971, pp. 164-167.

[*44*] Hochmann, J., *Revue de Metallurgie,* Vol. 48, 1951, pp. 734-758, (Brutcher Translation No. 2981).

[*45*] Demo, J. J., *Corrosion,* Vol. 27, 1971, pp. 531-544.

[*46*] Pruger, T. A., *Steel Horizons,* Vol. 13, 1951, pp. 10-12.

[*47*] Houdremont, E. and Tofaute, W., *Stahl und Eisen,* Vol. 72, 1952, pp. 539-545.

[*48*] Lula, R. A., Lena, A. J., and Kiefer, G. C., *Transactions,* American Society for Metals, Vol. 46, 1954, pp. 197-230.

[*49*] Bain, E. C., Aborn, R. H., and Rutherford, J. J. B., *Transactions,* American Society for Steel Treating, Vol. 21, 1933, pp. 481-509.

[*50*] Ebling, H. F. and Scheil, M. A. in *Advances in the Technology of Stainless Steels and Related Alloys, ASTM STP 369,* American Society for Testing and Materials, 1965, p. 275.

[*51*] Baumel, A., *Archiv für das Eisenhüttenwesen,* Vol. 34, 1963, pp. 135-149; British Iron and Steel Industry Translation No. 3287, London, 1963.

[*52*] Bond, A. P. and Lizlove, E. A., *Journal of the Electrochemical Society,* No. 116, 1969, pp. 1305-1311.

[*53*] Bond, A. P., *Transactions,* Metallurgical Society of the American Institute of Mining, Metallurgical, and Petroleum Engineers, No. 245, 1969, pp. 2127-2134.

[*54*] Demo, J. J., "Effect of High Temperature Exposure on the Corrosion Resistance and Ductility of AISI 446 Stainless Steel," NACE Preprint No. 23, 1968 Conference, Cleveland, National Association of Corrosion Engineers, 1968.

[*55*] Hodges, R. J., *Corrosion,* Vol. 27, 1971, pp. 119-127.

[*56*] Streicher, M. A., *Corrosion,* Vol. 29, 1973, pp. 337-360.

[*57*] Henthorne, M., *Localized Corrosion—Cause of Metal Failure, ASTM STP 516,* American Society for Testing and Materials, 1972, pp. 66-119.

[*58*] Mahla, E. M. and Neilsen, N. A., *Transactions,* American Society for Metals, Vol. 43, 1951, pp. 290-322.

[*59*] Streicher, M. A., *Corrosion,* Vol. 30, 1974, pp. 77-82.

[*60*] Semchyshen, M., Bond, A. P., and Dundas, H. J., *Toward Improved Ductility and Toughness,* Kyoto, Japan, 1971, pp. 239-253.

[*61*] Plumtree, A. and Gullberg, R., *Journal of Testing and Evaluation,* Vol. 2, No. 5, 1974, pp. 331-336.

[*62*] Gleiter, H. and Hornbogen, E., *Materials Science and Engineering*, Vol. 2, 1967/1968, pp. 285-302.

[*63*] Kinzel, A. B. and Franks, R., *The Alloys of Iron and Chromium, Vol. II—High Chromium Alloys*, McGraw Hill, New York, 1940.

[*64*] Legat, H., *Metallwirtschaft*, Vol. 17, 1938, pp. 509-513, (Brutcher Translation No. 654).

[*65*] Krivobok, V. N., *Transactions*, American Society for Metals, 1935, pp. 1-56.

[*66*] Heger, J. J., "The Effect of Notching on the Tensile and Impact Strength of Annealed 27% Chromium-Iron Alloy at Room and Elevated Temperatures," Report No. RR-3-6, The Babcock and Wilcox Tube Co., 28 March 1945.

[*67*] Lincoln, R. A., dissertation, Carnegie Institute of Technology, Pittsburgh, Pa., 1935.

[*68*] Hochmann, J., *Comtes Rendus*, No. 226, 1948, pp. 2150-2151.

[*69*] Binder, W. O. and Spendelow, H. R., *Transactions*, American Society for Metals, Vol. 43, 1951, pp. 759-777.

[*70*] Demo, J. J., *Transactions*, Metallurgical Society of the American Society of Mining, Metallurgical, and Petroleum Engineers, Vol. 5, 1974, pp. 2253-2256.

[*71*] Knoth, R. J., "Electron Beam Continuous Hearth Refining and Its Place in the Specialty Steel Industry," presented at the Specialty Steel Seminar, Pittsburgh, Pa., 1969.

[*72*] "E-Brite 26-1," Brochure No. AV110-3-71, Airco Vacuum Metals, Division of Air Reduction Co., Inc., Berkeley, Calif.

[*73*] Knoth, R. J., Lakso, G. E., and Matejka, W. A., *Chemical Engineering*, Vol. 77, No. 11, May 1970, pp. 170-176.

[*74*] Baumel, A., *Stahl und Eisen*, Vol. 84, 1964, pp. 798-802.

[*75*] Demo, J. J., "Ferritic Iron-Chromium Alloys," Canadian Patent No. 939,936, 15 Jan. 1974.

[*76*] Demo, J. J., "Ductile Chromium-Containing Ferritic Alloy," Canadian Patent No. 952,741, 13 Aug. 1974; patent applied for in the United States.

[*77*] Hersleb, G., *Werkstoffe und Korrosion*, Vol. 19, No. 5, 1968, pp. 406-412.

[*78*] Cowling, R. D. and Hintermann, H. E., *Journal of the Electrochemical Society*, Vol. 117, No. 11, 1970, pp. 1447-1449.

[*79*] Wright, R. N., *Welding Journal*, Research Supplement, Vol. 50, Oct. 1971, pp. 434s-440s.

[*80*] Pollard, B., *Metals Technology*, Jan. 1974, pp. 31-36.

[*81*] Sipos, D. J., Steigerwald, R. F., and Whitcomb, N. E., "Ductile Corrosion-Resistant Ferrous Alloys Containing Chromium," U.S. Patent No. 3 672 876, 27 June 1972.

[*82*] Bond, A. P., *Journal of the Electrochemical Society*, Vol. 120, No. 5, 1973, pp. 603-613.

[*83*] Steigerwald, R. F., "Low Interstitial Fe-Cr-Mo Ferritic Stainless Steels," Developments in the Field of Molybdenum-Alloyed Cast Iron and Steel, Soviet-American Symposium, Moscow, Jan. 1973.

[*84*] Steigerwald, R. F., *Tappi*, Vol. 56, No. 4, 1973, pp. 129-133.

[*85*] Steigerwald, R. F., "New Molybdenum Steels and Alloys for Corrosion Resistance," NACE Preprint No. 44, 1974 Conference, Chicago, National Association of Corrosion Engineers, 1974.

[*86*] Streicher, M. A., *Corrosion*, Vol. 30, No. 4, 1974, pp. 115-124.

[*87*] McMullin, J. G., Reiter, S. F., and Ebeling, D. G., *Transactions*, American Society for Metals, Vol. 46, 1954, pp. 799-811.

[*88*] Aggen, G., unpublished work, Allegheny Ludlum Industries, Inc., Pittsburgh, Pa.

[*89*] Demo, J. J., unpublished work, E. I. du Pont de Nemours and Co., Inc., Wilmington, Del.

[*90*] Schmidt, W. and Jarleborg, O., *Ferritic Stainless Steels with 17% Cr*, Climax Molybdenum GMBH, Dusseldorf, Germany, an affiliate of American Metal Climax, Inc., 1974.